Universidade de Aveiro Department of Materials and Ceramic Engineering

2018

BERNARDO NUNO GUERRA AMORIM

Exploração de Pneus Reciclados para Desenvolvimento de Novos Produtos

Exploration of Recycled Tires for Development of New Products

Universidade de Aveiro Department of Materials and Ceramic Engineering

2018

BERNARDO NUNO GUERRA AMORIM

Exploração de Pneus Reciclados para Desenvolvimento de Novos Produtos

Exploration of Recycled Tires for Development of New Products

Relatório de Projeto apresentado à Universidade de Aveiro para cumprimento dos requisitos necessários à obtenção do grau de Mestre em Engenharia de Materiais realizado sob a orientação científica da Doutoura Paula Celeste da Silva Ferreira, Equiparada a Investigadora Coordenadora do Departamento de Engenharia de Materiais e Cerâmica, coorientação da Doutoura Paula Maria Lousada Silveirinha Vilarinho, Professora Associada do Departamento de Engenharia de Materiais e Cerâmica da Universidade de Aveiro e do Doutor António Pedreiro, Diretor Geral da empresa RECIPNEU.

This work was developed within the scope of the project CICECO-Aveiro Institute of Materials, POCI-01-0145-FEDER-007679 (FCT Ref. UID /CTM /50011/2013), financed by national funds through the FCT/MEC and when appropriated co-financed by FEDER under the PT2020 Partnership Agreement

Por estarem sempre presentes em todas as etapas da minha vida, dedico este trabalho aos meus pais Ana e José.

o júri

presidente

Prof. Doutor João António Labrincha Baptista
Professor Associado no Departamento de Engenharia de Materiais e Cerâmica da Universidade de Aveiro

Prof. Doutor Victor Fernando Santos Neto
Professor Auxiliar no Departamento de Engenharia Mecânica da Universidade de Aveiro

Doutora Paula Celeste da Silva Ferreira
Equiparada a Investigadora Coordenadora do Departamento de Engenharia de Materiais e Cerâmica da Universidade de Aveiro

agradecimentos

Ao longo da minha formação, tive o privilégio de me cruzar com pessoas excecionais que sempre me ajudaram a crescer e a melhorar, quer profissionalmente quer pessoalmente.

Começo por agradecer às minhas orientadoras, Doutora Paula Ferreira e Professora Doutora Paula Vilarinho, pelo conhecimento científico, disponibilidade, dedicação e apoio ao longo da realização deste trabalho.

Agradeço ao Pedro Duarte, pelo conhecimento científico, disponibilidade e apoio incansável, ao longo da elaboração do trabalho.

A toda a equipa do Electroceramics Group e, em especial, ao Ricardo, André, Rui, Pedro, Manuela, Joana, Adriana, Nuno e João, pelo excelente ambiente de trabalho proporcionado, apoio e espírito de entre ajuda.

À Doutora Idalina Gonçalves, pelo apoio prestado durante a formulação dos compósitos.

Ao Professor Doutor Luís Godinho, pelo apoio técnico prestado na caracterização acústica das nossas amostras.

A toda a equipa do DEMaC, pelo apoio técnico prestado ao longo de toda a minha formação.

À minha namorada e aos verdadeiros amigos, por serem a minha segunda família, essencial para a concretização dos meus objetivos pessoais.

Aos meus padrinhos, Cátia e Rodrigo, pela amizade sincera e por serem uma inspiração.

Por fim, aos meus pais, Ana e José, por todos os ensinamentos, pela sincera amizade, apoio incansável e presença em todas as etapas da minha vida.

palavras-chave

Borracha, reciclagem, processo criogénico, termoplástico, extrusão de filamento, manufatura aditiva, painel acústico, economia circular

resumo

Estima-se que, em sociedades industrializadas, cerca de 9 a 10 Kg de pneus por habitante são, anualmente, descartados e despejados em enormes depósitos que acarretam sérios problemas ambientais. É de extrema importância reciclar pneus usados e desenvolver novas aplicações e novos produtos tendo por base os pneus reciclados. É precisamente este o enquadramento em que se realiza este trabalho de mestrado.

Neste trabalho, granulados de pneus reciclados, produzidos pela RECIPNEU, são incorporados em ácido poliláctico (PLA) de forma a preparar formulações de compósitos poliméricos para serem extrudidos em forma de filamento e serem, posteriormente, testados como material sustentável para manufatura aditiva de um painel acústico.

A preparação das formulações envolveu um estudo teórico prévio, baseado nas propriedades mecânicas e densidade, para definir a quantidade de granulados de pneus reciclados a ser incorporada. De seguida, formulações contendo 10 a 60 %, em peso, de granulados de borracha foram preparadas usando uma misturadora Brabender. Após extrusão dos filamentos com as diferentes formulações, verificou-se que o compósito contendo 20 %, em peso, de granulado de borracha foi o que apresentou a melhor homogeneidade, apesar da sua fragilidade. Adicionou-se um plasticizante, glicerol, de modo a melhorar a flexibilidade do filamento e permitir o seu enrolamento. As condições de extrusão foram otimizadas de modo a obter um filamento capaz de ser impresso, sendo este testado através da impressão de um pequeno protótipo de um painel acústico. As propriedades acústicas foram determinadas pelo Dr. Luís Godinho, Diretor do Departamento de Engenharia Civil da Universidade de Coimbra, através do método do tubo de impedância, e comparadas com uma amostra de PLA puro, de forma idêntica.

Resumindo, os granulados de pneus reciclados foram incorporados com sucesso em PLA, sendo possível extrudir os compósitos poliméricos em forma de filamento que pode ser usado como material sustentável para a manufatura aditiva.

É possível imprimir painéis customizados, contudo estes não apresentam boas propriedades acústicas, não sendo, na sua forma atual, uma boa solução para soluções acústicas. A percentagem de borracha necessita de ser otimizada, de modo a melhorar a performance acústica.

keywords

Rubber, recycling, cryogenic process, thermoplastic, filament extrusion, additive manufacturing, acoustic panel, circular economy

abstract

It is estimated that, in industrialized societies, over 9 to 10 Kg of tires per habitant are annually discarded and pilled in huge deposits with serious environmental problems associated. It is of maximum importance recycling used tires and developing new applications and new products of recycled tires.

In this work, recycled tire granulates, produced by RECIPNEU, are incorporated in polylactic acid (PLA) to prepare polymeric composite formulations to be extruded into a filament for sustainable additive manufacturing of an acoustic panel.

The preparation of the formulations involved a first theoretical/modelling study based on the mechanical properties and density to “guide” the establishment of the amount of recycled tire granulates to be included. Then, some formulations containing rubber percentages from 10 to 60 wt.% were prepared using a Brabender mixer.

Then, upon extrusion of the filaments with the different formulations, it was verified that the composite mixture containing 20 wt.% of rubber was the one presenting a higher degree of homogeneity despite its brittleness. A plasticizer, namely glycerol, was added to improve the filament flexibility and allow its rolling. A printable filament was obtained, and small prototypes of acoustic type panels were printed. Acoustic properties were determined in the laboratory of Professor Doctor Luís Godinho, director of the Department of Civil Engineering of the University of Coimbra, using the Wave Impedance Tube method, and were compared with similar shaped printed pure PLA.

Resuming, recycling tires waste were successfully incorporated in PLA and the polymeric composites could be extruded in filament form that can be used as a sustainable material for additive manufacturing.

The acoustic performance of the printed panels, tested by Wave Impedance Tube method, revealed an inferior performance when compared with standard mineral wool sample, being necessary to perform more studies in this field.

Index

List of Figures…… iii

List of Tables…….. vi

List of Abbreviations…….. ix

1. Introduction…… 1

1.1. Tire…… 3
1.2. Tire Composition…… 4
1.3. Tire Vulcanization…… 5
1.4. Problem…… 6
1.5. Tires Recycling…… 7
1.5.1. Mechanical Process…… 8
1.5.2. Cryogenic Process…… 9
1.6. RECIPNEU…… 13
1.7. Acoustic Applications…… 14
1.8. Sound Absorption…… 17
1.9. Additive Manufacturing…… 18
1.10. Objectives…… 25

2. Experimental Procedure…… 27

2.1. Raw materials characterization…… 29
2.1.1. SEM/EDS…… 29
2.1.2. FTIR…… 31
2.1.3. DSC/TGA…… 32
2.2. Formulation of the composite…… 33
2.3. Filament Extrusion of the composite…… 35
2.4. Additive Manufacturing…… 37
2.5. Density Determination…… 39
2.6. Acoustic characterization…… 39

3. Results and Discussion…… 43

3.1. Theoretical prediction of the composites behavior…… 45
3.2. Raw material characterization…… 49
3.2.1. SEM/EDS …… 50
3.2.2. FTIR…… 52
3.2.3. DSC/TGA…… 53
3.3. Preparation of the formulation of the composite…… 54
3.4. Filament extrusion and characterization…… 57
3.5. Additive Manufacturing…… 62
3.6. Density Determination…… 68
3.7. Acoustic characterization…… 68

4. Conclusions and Future Work…… 71

5. References…… 77

List of Figures

Figure 1.1 – Tire cross section according to Michelin [1]. The tire is divided in 7 different critical parts: the inner liner (1), the casing (2), the apex (3), the bead (4), the sidewalls (5), the belts (6) and the tread (7). ……..3

Figure 1.2 – Chemical structures of: a) polyisoprene and b) styrene-butadiene rubber [2,3]. ……..5

Figure 1.3 – Schematic representation of the crosslinking of a vulcanized natural rubber polymer chains [4].……6

Figure 1.4 – Typical ambient mechanical grinding process scheme [9]. The process starts with the raw material (a), that will pass through 3 machines: a shredder (b), a fabric separator (c) and a mill (d). In the system, also are present: a reclaimer (e), two sifting screens, (f) and (g), bagging (h), baller (i) and shipping (j). ……8

Figure 1.5 – Surface morphology of rubber particle obtained by ambient mechanical grinding [10]. The particles obtained by this recycling method present a “spongeous” type morphology. ……..9

Figure 1.6 – Typical cryogenic grinding process diagram [8]. The cryogenic processing encompasses 8 different steps: a) preliminary shredder, b) freezing tunnel, c) hammer mill, d) steel and fiber removal, e) dryer, f) classifier, g) secondary grinding step and h) product storage silos. ……..10

Figure 1.7 – Surface morphology of a cryogenic rubber particle [7]. ……..11

Figure 1.8 – Common applications of the cryogenic recycled rubber granulate: a) horse riding tracks; b) low-noise road pavements; c) rubber infilling for artificial turf football fields and d) playgrounds for children [13]. ……14

Figure 1.9 – Simplified diagram of the FDM technique: 1- filament spool, 2- filament, 3- extruder, 4- heater block, 5- nozzle, 6- piece and 7- bed [24]. The filament is led into the extruder, melting and being extruded into the bed, in the desired x/y/z position. ……21

Figure 1.10 – Process and Life cycle of PLA [28]. ……23

Figure 2.1 – Different signals generated from the interaction between the electron beam and the sample. (adapted from [30]). ……...30

Figure 2.2 – FTIR equipment. In this technique, infrared radiation passes through the sample, being absorbed or transmitted. The measured signal is accomplished by Fourier transformation (performed by a computer) and a frequency spectrum is obtained. ……...31

Figure 2.3 – DSC interpretation of a polymeric material [36,37]. DSC measures the energy absorbed or produced as a function of time or temperature and is used to characterize melting, crystallization, curing, loss of solvents and other processes involving an energy change and changes in heat capacity. ……...32

Figure 2.4 – Brabender mixer equipment [39]. In this equipment, the raw material is homogenized by specially shaped mixing blades, in the previously heated mixer bowl. ……34

Figure 2.5 – 3devo NEXT Extruder [35]. This equipment was used to extrude into a filament form the different composite compositions. ……..35

Figure 2.6 – Scheme of the extrusion process. The mixture was pushed through 4 heating zones (T_4, T_3, T_2 and T_1) by a nitride hardened steel extruder screw, operating at 5 rpm…….36

Figure 2.7 – Anet A8-B 3D printer (left). Extruder nozzle ampliation (right). (adapted from [50]). ……37

Figure 2.8 – Schematic representation of the Archimedes' Principle performed to determine the density of both samples A1 and A2. ……39

Figure 2.9 – Scheme of the standard test method for Impedance and Absorption of Acoustical Materials [43]. ……..39

Figure 2.10 – G.R.A.S. 46 E microphones. ……40

Figure 2.11 – NI USB 4431 device. ……...41

Figure 2.12 – Setup of the wave impedance tube. ……42

Figure 3.1 – Theoretical prediction of the composites behavior: a) tensile strength, b) yield strength, c) Young modulus, d) density and e) compressive strength, as function of the rubber granulate (% V). The mechanical properties of the PLA matrix decreased with the rubber addition, reaching a minimum for 10 % in volume, being almost constant higher percentages. The composites' density was constant until around 20 % in volume, perceiving a substantial decrease between 20 and 30 % in volume, evidencing a slight increase of this value for increasingly high rubber percentages. ……48

Figure 3.2 – SEM micrographs of DC-8000. The grains obtained present irregular rectangular shapes, a flat morphology, and a relative smooth surface, typical characteristics. ……49

Figure 3.3 – EDS analysis of DC-8000 sample. Carbon, sulfur, silica, zinc, oxygen, calcium, aluminum and iron were identified as the main components of these rubber granulates. …….50

Figure 3.4 – Rubber sample (DC-8000) FTIR analysis. The vibrations detected correspond to the functional groups present in the tires such the ones assigned to the rubber and functional groups related with rubber vulcanization. ……51

Figure 3.5 – DSC/TG analysis of the cryogenic rubber granulates (DC-8000). The recycled tires granulate is almost stable until 300 °C. Above 300 °C and up to 500 °C a huge drop of mass around 60 % is visible. At 365 °C is visible an exothermic peak related with the initiation of the decomposition of the rubber granulates. At 420 °C, there is an endothermic peak considered to be caused by partial oxidation of carbon black. ……52

Figure 3.6 – Different composite mixtures tested: a) 10 wt.% rubber; b) 20 wt.% rubber; c) 40 wt.% rubber; d) 60 wt.% rubber; e) 20 wt.% rubber + 2 wt.% glycerol. The highest rubber percentages tested (40 and 60 wt.%) were brittle, while the lowest rubber percentages tested (10 and 20 wt.%) were stiff). Mixture 20 wt.% rubber + 2 wt.% glycerol turned liquid but presented a fast solidification. ……...55

Figure 3.7 – Different composite mixtures extruded into filament form: a) 10 wt.% rubber; b) 20 wt.% rubber; c) 40 wt.% rubber; d) 60 wt.% rubber; e) 20 wt.% rubber + 2 wt.% glycerol (filament F1). Filament F1 was chosen to be applied in additive manufacturing. ……56

Figure 3.8 – Variability of the filament F1 diameter extruded with spooling on. This study was performed by measuring the filament diameter every 2 cm. This filament presented a mean value of 1.17 mm of diameter and a median value of 1.16 mm. ……58

Figure 3.9 – Filament F2 extruded with spooling off: a) manual extrusion and b) final filament. ……59

Figure 3.10 – Variability of the filament F2 diameter extruded with spooling off. This study was performed by measuring the filament diameter every 2 cm. This filament presented a mean value of 1.97 mm and a median value of 1.96 mm. ……60

Figure 3.11 – The first printing attempts were an 8 cm^3 cube. Different temperatures and nozzle diameters were tested: a) T=190 °C, 0.8 mm nozzle; b) T=180 °C, 0.8 mm nozzle; c) T=170 °C, 0.8 mm nozzle; d) T=170 °C, 0.6 mm nozzle; e) T=170 °C, 0.6 mm nozzle. The most suitable parameters were defined as T=170 °C and a 0.6 mm nozzle diameter, ensuring a continuous printing. ……61

Figure 3.12 – CAD model of the “egg box type” panel designed with a quadrangular base of 5 cm side, with four quadrangular pyramids of 1 cm of height. ……62

Figure 3.13 – First printing attempt of an “egg box type” panel designed with a quadrangular base of 5 cm side, with four quadrangular pyramids of 1 cm of height. Panel printed with filament F2, with a 0.6 mm nozzle diameter and an extrusion temperature of T = 170 °C. ……62

Figure 3.14 – “Egg box type” panel designed with a quadrangular base of 5 cm side, with four quadrangular pyramids of 1 cm of height. Panel printed with filament F2, with a 0.6 mm nozzle diameter and an extrusion temperature of T = 170 °C. ……63

Figure 3.15 – CAD model of samples A1 and A2. Round flat samples with 5 cm of diameter and 3 cm of height. ……64

Figure 3.16 – CAD model of sample A3. Round sample with “egg box type” topography with 5 cm diameter and 3 cm of height. ……...64

Figure 3.17 – Sample A1 – Flat PLA sample. ……66

Figure 3.18 – Sample A2 – Flat sample printed with filament F2. ……66

Figure 3.19 – Sample A3 – “Egg box type” sample printed with filament F2. ……66

Figure 3.20 – Comparison between the acoustic absorption results of samples A1, A2 and a mineral wool sample (example of an absorbent material). A tridimensional structure with porosity is necessary to improve the absorption coefficient value of our samples. ……68

Figure 3.21 – Comparison between the acoustic absorption results of samples A1, A2 and a mineral wool sample (example of an absorbent material). A tridimensional structure with porosity is necessary to improve the absorption coefficient value of our samples. ……69

List of Tables

Table 1.1 – Generic composition of tires [2]. Tires are mainly composed by rubber, carbon black, silica, metals, textile fibers and processing additives. ……..4

Table 1.2 – Comparison between Cryogenic and Ambient rubber granulates [10]. ……..12

Table 1.3 – Absorption coefficients of general building materials and furnishings [21]. ……18

Table 1.4 – Additive manufacturing different techniques comparison [23]. ……...20

Table 2.1 – Different mixture compositions and parameters tested in the BRABENDER mixer. Mixtures of PLA and rubber were prepared, with rubber percentages, in mass, between 10 and 60%. A rubber percentage of 20 wt.% was also tested with the addition of glycerol as a plasticizer. ……34

Table 2.2 – Naming of the filaments used in the additive manufacturing. ……36

Table 2.3 – Naming and characteristics of the round printed samples. ……38

Table 3.1 – Specifications of the different types of granulates provided by RECIPNEU [13]. DC-8000 sample was selected because of its lower nominal dimensions. ……49

Table 3.2 – RECIPNEU's information about the composition of the cryogenic rubber granulates [10]. ……...50

Table 3.3 – Different mixture compositions and parameters tested in the BRABENDER mixer. Mixtures of PLA and rubber were prepared, with rubber percentages, in mass, between 10 and 60%. A rubber percentage of 20 wt.% was also tested with the addition of glycerol as a plasticizer. ……55

Table 3.4 – Experimental observations of the different composite formulations tested. ……57

Table 3.5 – Identification and characteristics of the printed samples (A1, A2 and A3) for acoustic characterization. ……..64

List of Abbreviations

SEM/EDS	Scanning Electron Microscopy / Energy-Dispersive X-ray Spectroscopy
FTIR	Fourier-Transform Infrared Spectroscopy
DSC/TGA	Differential Scanning Calorimetry / Thermogravimetric Analysis
FDM	Fused Deposition Modelling
CAD	Computer-Aided Design
STL	Standard Tessellation Language
PLA	Poly-lactic Acid
PE	Polyethylene
PC	Polycarbonate
SBR	Styrene Butadiene Rubber
NR	Natural Rubber

1. INTRODUCTION

1. INTRODUCTION

Serious environmental problems are created of discarded tires that are piled in huge deposits, being mandatory the recycling of used tires and the developing of new applications and new products for their correct reutilization, promoting a circular economy.

1.1. Tire

A tire is a large, round, black hollow shell filled with compressed air that is scrupulously constructed to meet different performance standards. The structure of a tire is divided in 7 different critical parts: the inner liner, the casing, the apex, the beads, the sidewalls, the belts and the tread, as illustrated in Figure 1.1. [1] [2]

Figure 1.1 – Tire cross section, according to Michelin [1]*. The tire is divided in 7 different critical parts: the inner liner (1), the casing (2), the apex (3), the bead (4), the sidewalls (5), the belts (6) and the tread (7).*

The inner liner (1) is an airtight layer of synthetic rubber that is located inside the tire and works as an air chamber. It provides a lining for the casing to maintain consistent pressure and to contain the air, improving rolling resistance and energy savings. The casing (2) is a flexible structure made up of filaments (textiles or steel) embedded in the rubber which form straight arcs and roll onto the bead of the tire. On the casing, are placed the rest of the belts and rubber layers that form the tire. The casing is responsible for bearing stress and providing the shape and internal structure of the tire. The apex (3), has the role of transmitting the engine torque

(vehicle power), in acceleration and braking, from the rim to the contact zone with the ground. The bead (4) is the part of the tire that anchors the tire to the wheel rim. The sidewalls (5) reinforce the interface between the tire and the wheel rim and set the inner dimension, contributing to the structural integrity of the tire. The different roles of the sidewalls are: to support load, to withstand the constant mechanical flexures, to resist to frictions and aggressions and to participate in stability and comfort. The belts (6), that are place on the bias at alternate angles under the tread, provide structural support to the tread and help maintaining the tire shape. They consist of metal filaments coated with rubber, and they are positioned on the casing forming a waist that guaranties the mechanical resistance of the tire to the speed and centrifugal force. The tread (7) is the exterior part of the tire that is directly in contact with the road. This part of the tire is designed in such a way that the solid parts of the tread clear away the water and the channels allow the water to flow outwards. This way, the tread can maintain contact with the surface. Its functions are: provide grip on both wet and dry soil, duration and resistance to wear and tear, participate in acoustic comfort (rolling sound), participate in the steering and maneuverability of the vehicle and, also, aesthetics. [1] [2]

1.2. Tire Composition

Tires are mainly composed by rubber, carbon black, silica, metals, textile fibers and processing additives as shown in Table 1.1. [2]

Table 1.1 - Generic composition of tires [2]. *Tires are mainly composed by rubber, carbon black, silica, metals, textile fibers and processing additives.*

Material	Composition (wt.%)
Rubber	43
Carbon Black/Silica	27
Metals	11
Textiles	5
Vulcanization Aids	3
Additives	3
Aromatic Oils	8

The main components of tires composition are natural (NR) and synthetic rubbers (usually SBR). The second material with the highest percentage is carbon black and/or silica, that can be used in several different parts of the tire: inner liner, casing or even the tread. Metals and textiles are also presented in the tires composition, working as reinforcing materials. Aromatic oils' role is to facilitate the processing of the rubber compounds and to improve the technical performance of the tires. [2]

After the addition of all these components and the assembling of the tire structure, the tire is vulcanized.

1.3. Tire Vulcanization

A rubber is an elastomeric compound that consists of long chains of molecules that are tangled up and only weakly linked together, without crosslinking between them, being relatively easy to pull them apart. Rubber, at this stage, is soft, sticky, has low tensile strength and is thermoplastic. [2] [3]

Back in 1839, Charles Goodyear, developed the vulcanization process by mixing, accidently, natural rubber (polyisoprene) and sulfur with other ingredients in a hot stove and, noticed, that the rubber had become a tough and firm material. Over the years, many synthetic rubbers (SBR, for example) have also been introduced as components of vulcanization systems. [2] [3] In Figure 1.2, are represented the chemical structures of polyisoprene (a) and SBR (b).

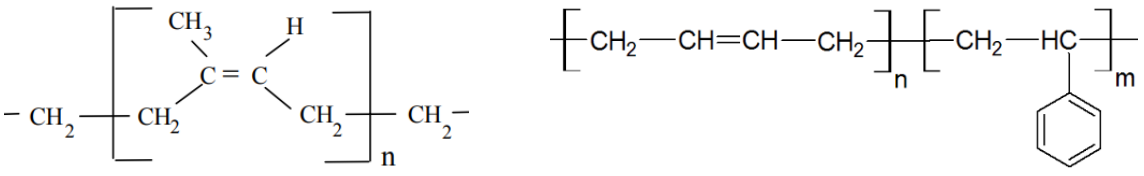

Figure 1.2 – Chemical structures of: a) polyisoprene and b) styrene-butadiene rubber. [2] [3]

During the vulcanization process, the added sulfur atoms will react with the carbon double bonds of both polyisoprene and SBR to form crosslinking between the polymer chains, tying the molecules together and making them much harder to

pull apart. The crosslinking introduced by the vulcanization process, prevents the polymer chains to move independently and, as a result, when stress is applied the rubber suffers deformation, however, upon the stress release it acquires its original shape. Figure 1.3 represents a schematic representation of the crosslinking of a vulcanized natural rubber polymer chains. [2] [3] [4]

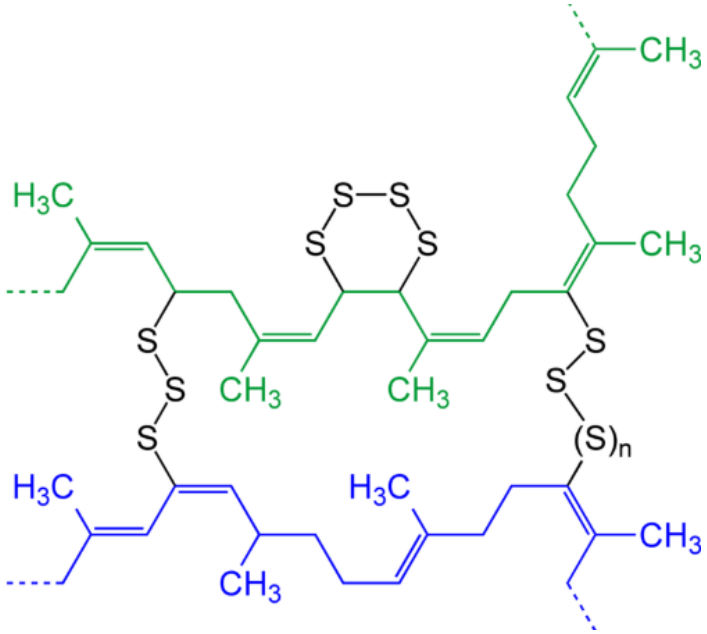

Figure 1.3 - Schematic representation of the crosslinking of a vulcanized natural rubber polymer chains [4].

1.4. Problem

One of the biggest challenges for the 21st century is the development of the necessary tools to avoid waste in large scales, namely of both plastic and rubber, mainly due to their long decomposition time, the damages that they cause to the animal life and to the technical difficulties in reutilize them.

It is estimated that, in industrialized societies, annually, over 9 to 10 Kg of tires per inhabitant are discarded and piled in huge deposits. These deposits create serious environmental problems: firstly, in case of a fire, the fires are very hard to extinguish and there is the release of extremely toxic compounds; secondly, they accumulate water puddles in their interior, resulting from the rain, that will lead to the procreation of mosquitos, major diseases propagation agents. [5]

At the moment, the available solutions for used tires are: retread, recycling, energy recovery and reuse for other purposes. [6]

Tire retread is process that transforms used tires (carcasses) that do not show any structural damage, into that can be reused, through the application of a new tread. In the past year, 2017, around 14 % of used tires were sent to retread. [6]

Concerning energy recovery, used tires can be used as an additional or alternative fuel for cement production or to produce electricity and steam in cogeneration units, due to its high heating power, which is around 5700 Kcal/Kg. In the past year, around 25 % of used tires were sent for energy recovery. [6]

Used tires can also be used for other purposes, as: protection for marine piers, boats, permeable surfaces for roads, etc. For these purposes, only around 1 % of used tires were sent, in the past year. [6]

Concerning recycling of used tires, in the past year, around 60 % of used tires were sent for recycling. [6]

It is mandatory recycling used tires and developing new applications based on their correct reutilization for a wide range of uses, and adding value, based on knowledge and technology, to the development of products of recycled tires.

Over recent years, significant investments have been made in order to develop new end markets and added value applications for the recycled tires, combining them with an environmental friendly behavior. [7]

1.5. Tires Recycling

Considering that tires have a complex matrix constituted, in its majority, by vulcanized rubber, thermoset, that does not melt and that gets decomposed when heated above 300 °C, its recycling is a challenge. Nowadays, its mechanical trituration is performed for further utilization.

The recycling of used tires can be made by two different processes: mechanical or cryogenic process. In this section these processes and their main differences will be described.

1.5.1. Mechanical Process

The mechanical process consists in the mechanical trituration of the tires. In an ambient system, the rubber, tires or other feedstock remain at room temperature as they enter the granulator. [8]

Ambient grinding is a multi-step processing technology that uses three machines, to separate the rubber, metal and textiles. The first processing step reduces the original feedstock to small chips. The second machine will grind the chips and the metals are magnetically separated out. Then a finishing mill will grind the material to the required product specification. After each processing step, the material is classified by sifting screens that return oversize pieces to the granulator or mill for further processing. In the final stage, textile residues are removed by air separators. [8]

A schematic representation of the mechanical recycling process is presented in Figure 1.4. [9]

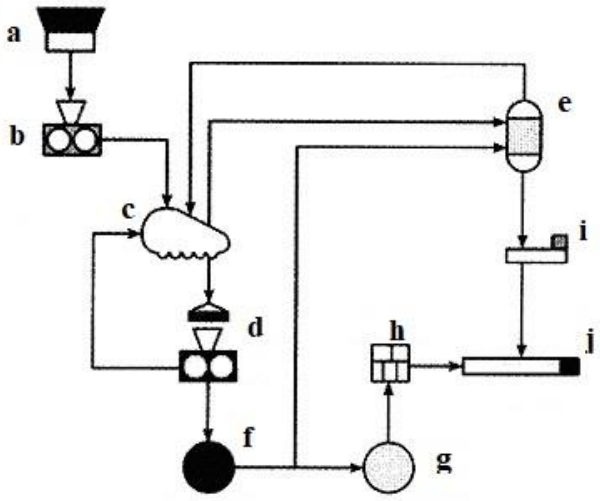

Figure 1.4 – Typical ambient mechanical grinding process scheme [9]*. The process starts with the raw material (a), that will pass through 3 machines: a shredder (b), a fabric separator (c) and a mill (d). In the system, also are present: a reclaimer (e), two sifting screens (f) and (g), bagging (h), baler (i) and shipping (j).*

The resultant particles of this process, present reasonable ageing resistance, good resistance to UV radiation and regular elastic properties, however they also present some serious disadvantages like: poor compaction resistance, bad rain water drainage, lower apparent density, high amount of inhalable dust liberation, intense rubber smell and even adherence to skin and clothes. The particles obtained also present a “spongeous” type morphology (very high pore density and very high superficial area per unit mass), as shown in Figure 1.5. [10]

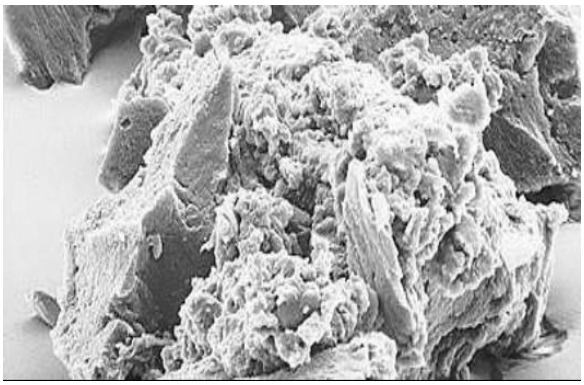

Figure 1.5 - Surface morphology of rubber particle obtained by ambient grinding [10]. *The particles obtained by this recycling method present a “spongeous” type morphology.*

1.5.2. Cryogenic Process

Cryogenic processing refers to the use of liquid nitrogen to freeze the tire chips or rubber particles prior to size reduction. Most rubber become embrittled or “glass-like” at temperatures below $-196°C$. The use of cryogenic temperatures can be applied at any stage of size reduction of scrap tires. The material can be cooled in a tunnel style chamber, immersed in a bath of liquid nitrogen, or sprayed with liquid nitrogen to reduce the temperature of the rubber or tire chip. It is a 4-phase system, including: initial size reduction, cooling, separation and milling. Since the rubber is embrittled, it is possible to fracture it to the desired size, what results in a smooth and regular shape. [8]

Figure 1.6 is a schematic representation of this process.

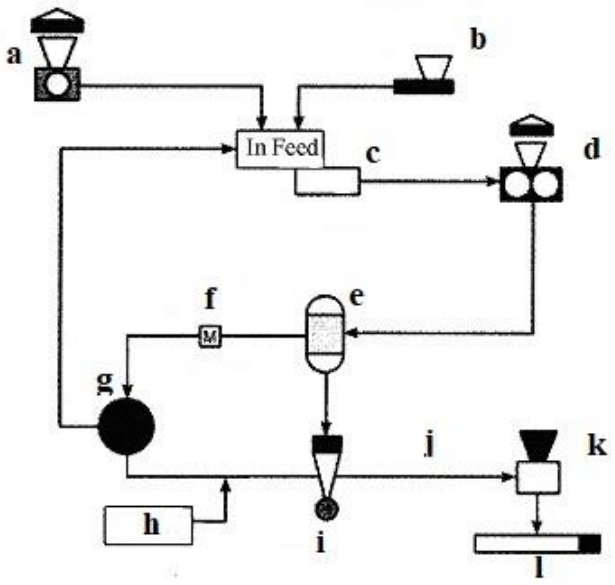

Figure 1.6 – Typical cryogenic grinding process diagram [8]*. The cryogenic processing encompasses 8 different steps: a) preliminary shredder, b) freezing tunnel, c) hammer mill, d) steel and fiber removal, e) dryer, f) classifier, g) secondary grinding step and h) product storage silos.*

The process begins with shredding the raw material into small chips, with a size between ~10 mm and ~50 mm. The chips are then dropped into a long cryogenic tunnel and cooled by liquid nitrogen to – 196°C, surpassing the glass-transition point of the tire rubber polymers. The chips are then hit by hammer mills, causing the instantaneous fracture of the “glassy” rubber chips into small rubber granulates. The granulates then pass through a series of magnetic screens and sifting stations to remove the last trace elements of impurities. In this process no degradations are introduced in the rubber, neither thermal nor chemical-oxidative. [10]

The cryogenic rubber granulates have a flat morphology, as shown in Figure 1.7 with a smooth surface, with practically no pores. Due to the absence of pores at the surface, the specific surface is minimal and the release of rubber constituents to the exterior is very reduced. This rubber does not flow in water. [10]

These granulates obtained have long durability under strong UV radiation due to minimal volatiles released, adding to this their minimal leachates and odour release. [10]

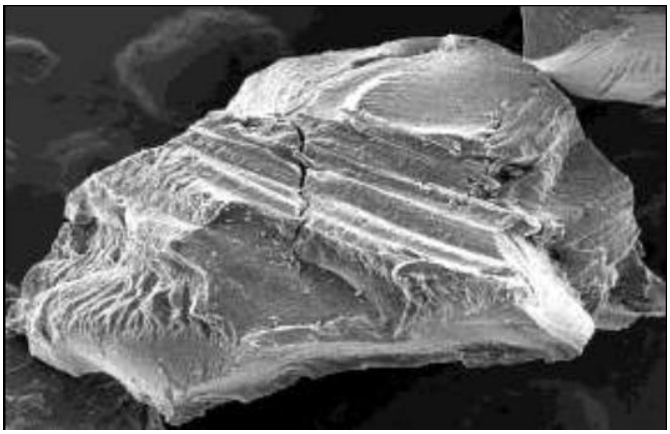

Figure 1.7 - Surface morphology of a cryogenic rubber particle [7].

Cryogenic rubber particles have irregular solid shapes and besides that they are an excellent water drainer, they don't compact (due to its good abrasion resistance), they show a prompt elastic recovery (due to the non-degraded rubber polymer chains) and they have a good shock absorption. [10]

The cryogenic rubber granulates are also health and environmental friendly, because they have no rubber smell, do not release black powder, have high stability in place and have negligible release of inhalable particles. [10] Table 1.2 compares the rubber granulates obtained by these two different recycling methods.

Table 1.2 – Comparison between Cryogenic and Ambient rubber granulates. [10]

Cryogenic Rubber Granulates	Ambient Rubber Granulates
Rubber particles with flat surface morphology (low pore density)	Particles with “spongeous” type morphology (very high pore density)
Particles with irregular shape, round to moderately angular	Particles with very irregular shape
Excellent compaction resistance (rubber does not compact during the years of use)	Poor compaction resistance (rubber compacts during the years of use)
Excellent rain water drainage	Bad rain water drainage
Excellent ageing resistance	Reasonable ageing resistance
Excellent resistance of the rubber particles to UV radiation	Good resistance of the rubber particles to UV radiation
Excellent elastic properties (molecular structure not degraded)	Regular elastic properties (molecular structure much degraded)
Practically no rubber smell	Intense rubber smell
No release of abraded carbon black (no staining / no adherence to skin and clothes)	Staining / adherence to skin and clothes

According to the literature, cryogenic rubber granulates are also excellent sound absorbers if the size of the aggregate and the binder content its carefully selected. Acoustic paneling made of elastic granular materials can be an improvement on conventional sound absorbers because of their ability to combine both the conventional visco-thermal mechanism of sound absorption and the structural damping effect. [11] [12]

This last property of the cryogenic rubber granulate leads us to another factor that, nowadays, affects the human health and the environment, the noise and the necessity to control it.

The main drawback of this recycling process is the higher cost, when compared to the mechanical one, however it leads to added value rubber granulates.

1.6. RECIPNEU

RECIPNEU, a Portuguese company located in Sines, specialized in recycling tires, approached the University of Aveiro with the need of an added value application for the high quality recycled tires rubber granulates that they are producing.

RECIPNEU company produces rubber granulates from recycling end-of-life tires since the year 2000 by a cryogenic process, providing high quality rubber granulates for applications as raw material or final product. [13]

The main aim of RECIPNEU is the production of high quality cryogenic rubber granulates and the valorization of all the components that result from the recycling of end-of-life tires as well as their use in valuable applications with great use for the current market. [13]

RECIPNEU is currently responsible for recycling around 40% of the end-of-life tires produced in Portugal, being one of the main players for end-of-life tires valorization in Portugal. [13]

RECIPNEU is currently one of the few European producers offering cryogenic rubber granulates. The company exports its products to countries ranging from the USA to Russia, countries in the Middle East and Africa. Exports represent 60% of RECIPNEU's sales. [13]

The cryogenic granulates produced by RECIPNEU are used for different applications (Figure 1.8), as: rubber infilling for artificial turf football fields, low- noise road pavements, horse riding tracks, playgrounds for children and raw material for the polymer-processing industry. [13]

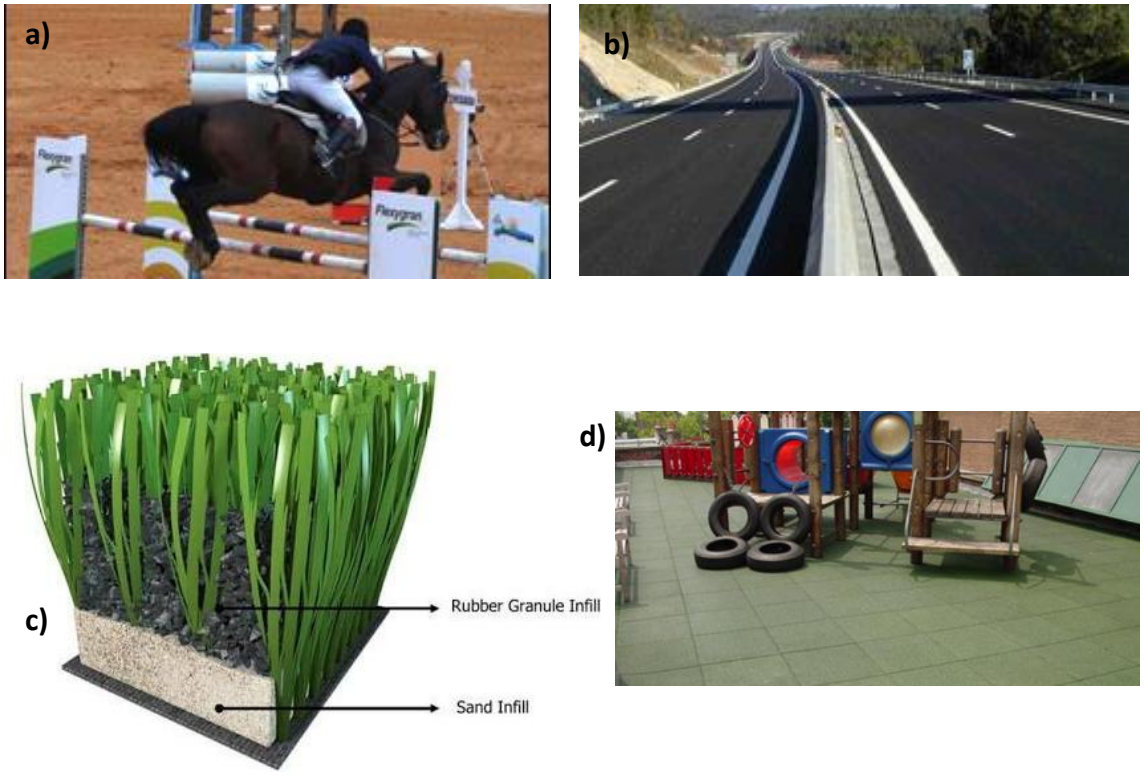

Figure 1.8 – Common applications of the cryogenic recycled rubber granulate: a) horse riding tracks; b) low-noise road pavements; c) rubber infilling for artificial turf football fields and d) playgrounds for children. [13]

Within this context, in this work, the development of polymeric composites with recycled tires rubber granulates to be used in the fabrication of customized products by additive manufacturing, as for example, acoustic panels, is explored.

1.7. ACOUSTIC APPLICATIONS

With the development of modern industry and traffic system, noise has become one of the major factors affecting human health and environment worldwide, so it is of maximum importance to reduce noise and to avoid the damages caused by noise. [14]

Noise can be controlled by: i) reducing the sources of noises through the building facilities which produce less or no noise at all (effective method), ii) using sound absorption and iii) applying sound insulation materials to eliminate or reduce the sound wave on its way of transmission. [14]

In the recent years, several studies have been carried out to develop new materials and technologies improving the sound absorption properties. [14]

New insulating solutions with recycled materials are becoming more common on the market. Recycled materials are considered environmental friendly because they are produced from discarded waste materials/components and represent an excellent alternative, allowing the reduction of the quantity of waste to be treated. [15]

Zhou *et al.* [16] found that recycled rubber particles had some excellent sound energy absorbency properties and the composite panel made with recycled rubber crumbs created some good sound attenuation. The sample preparation consisted of a composite with a layer upon layer structure with the rubber particles as bottom layer, on the top of which is single or multiple layer of polymer porous foam or perforated panel. The sound absorption measurement was performed with a two-microphone impedance tube (type 4206) of Bruel&Kjaer (B&K) according to the standard procedure detailed in ISO (10534-2) and with a frequency range between 100 and 1600 Hz. Firstly, the double-layer structure of rubber particles layer, on top of which is laminated PU, has been studied, and two different samples were tested: U1 (foam thickness, 5 mm) and U2 (foam thickness, 10 mm). The maximum value of absorption coefficient obtained for sample U1 was 0.38, while for sample U2 was 0.45. Secondly, the double-layer structure of rubber particles with perforated panel was studied and two different samples were performed: A2 (3 mm thickness, 5 mm pore size and 4.75% porosity) and C1 (3mm thickness, 3 mm pore size and 1.17% porosity). The maximum value of absorption coefficient obtained for sample A2 was 0.65, while for sample C1 was above 0.9. Lastly, two samples of a multi-layered structure composed by an assembly between a perforated panel A2, rubber particle of 150 μm and porous materials (PU foam of 40 kg/m^3, CP21, and glass wool of 103.59 kg/m^3, CP22). The maximum value of absorption coefficient obtained for CP21 was greater than 0.9, while the sample CP22 presented a maximum absorption coefficient of exactly 0.9.

Yang *et al.* [17] studied the straw-waste tire composites and their test results showed that straw/recycled tire rubber composites had similar mechanical

properties compared to wood/recycled tire rubber composites, however the first one possessed better sound insulation. Samples of 30 wt.% random cut rice straws, without size screening, were performed and tested to investigate the possibility of these being used as insulation materials and insulation boards in construction. The sound absorption coefficient was determined by impedance tube method (ASTM C 384-98, American Society for Testing and Materials, 1999) in a frequency range between 125 and 8000 Hz. The absorption coefficient of the composite boards increased as the frequency increased, however it decreased around a frequency of 1000 Hz and, then, increased again until a maximum value of 0.5.

Maderuelo-Sanz *et al.* [18] studied the use of material waste (ground end of life tires) in the manufacture of sound absorber products, concluding that this kind of waste had good acoustic properties at both low and high frequencies. The purpose of their study was to show the acoustic properties of materials made with fluff (composed of an elastomeric nature waste named ground tire rubber (GTR), loose and consolidated, textile and metal fibres), both with and without resin. Circular samples, with 100 mm and 29 mm in diameter, of these composite materials, composed of two layers (one of GTR and another made of fluff) were analysed with the impedance tube, where the measurements of the larger sample was performed over the range of frequencies from 50 Hz to 1.6 kHz, while the smaller one was performed over the range of frequencies from 500 Hz to 6.4 kHz. The acoustic properties of the samples were measured using a two-microphone impedance tube (Brüel & Kjær, type 4206) and two ¼ "Condenser microphones type 4187, according to the standard procedure detailed in ISO 10534-2, in the frequency range of 100 to 6400 Hz. As result of their study, they concluded that this kind of waste has good acoustic properties, at both low and high frequencies, reaching an absorption coefficient maximum value of 0.99 in some of their tested samples. The samples with resin in their composition showed a lower value of absorption coefficient.

The acoustic characteristics are extremely important in building design and in layouts of residences, plants, offices and institutional facilities, because it provides adequate insulation against outside noises from transportation and other sources. For example, interior walls and partitions need to be designed to prevent the

intrusion of sound from one room into another. Exposure of workers to excessive occupational noises can be decreased by the construction of adequate barriers or enclosures around the noisy machinery. Excessive noise from highways/railroads can be decreased by implementation of sound barriers. [19]

1.8. SOUND ABSORPTION

The term “sound” stands for mechanical oscillations with wave-like propagation, and sound waves can propagate in air, liquids or in solid bodies.

Acoustics is the science of sound and deals with the generation of sound, propagation and interaction with matter and also the perception by humans. [20]

In enclosed spaces, the distribution of acoustic energy, whether originating from a single or multiple sound sources, depends on the room size and geometry and on the combined effects of reflection, diffraction and absorption.

All materials constituting the boundaries of an enclosure will absorb and reflect sound. A fraction α, of the incident energy, is absorbed and the balance $(1 - \alpha)$ is reflected. Reflection is indicated by the reflection coefficient, r, defined as in Equation 1.1,

$$r = \frac{amplitude\ of\ reflected\ wave}{amplitude\ of\ incident\ wave}\ [19] \qquad \text{(Equation 1.1)}$$

Because the energy, in a sound wave, is proportional to the square of the amplitude, the sound absorption coefficient, α, and the reflection coefficient, r, are related by the Equation 1.2,

$$\alpha = 1 - r^2\ [19] \qquad \text{(Equation 1.2)}$$

The absorption coefficient varies with the angle at which the wave strikes the material and with the frequency, so it is common practice to list values at specific frequencies in tables of absorption coefficients, usually at 125, 250, 500, 1000, 2000 and 4000 Hz.

Table 1.3 presents the absorption coefficients of some general building materials and furnishings. [21]

Table 1.3 - Absorption coefficients of general building materials and furnishings [21].

Materials	Absorption Coefficient (α)					
	125 Hz	250 Hz	500 Hz	1000 Hz	2000 Hz	4000 Hz
Brick, unglazed	0.03	0.03	0.03	0.04	0.05	0.07
Carpet, heavy, on concrete	0.02	0.06	0.14	0.37	0.60	0.65
Concrete block, coarse	0.36	0.44	0.31	0.29	0.39	0.25
Wood floor	0.15	0.11	0.10	0.07	0.06	0.07
Ordinary window glass	0.35	0.25	0.18	0.12	0.07	0.04

The absorption coefficient depends not only on the nature of the material but also on other factors such as its thickness, on the way in which it is mounted, and on the depth of the air space behind it. [21]

Currently, there are two different experimental methodologies normalized that allow the determination of the sound absorption coefficient of materials. One of these methodologies, defined in the ISO 354, consists in the realization of tests in a reverberation chamber, in diffused field conditions, over samples with around 10 m^2. Although this method is of general application, it requires the utilization of large amounts, becoming unpractical. As an alternative to this method, comes up the procedure described in the ASTM E 1050 that allows the determination of the sound absorption coefficient of a material when it is subjected to a normal incidence of sound waves through measurements performed in an impedance tube. [21]

1.9. ADDITIVE MANUFACTURING

Acoustic panels need to have a well-defined design and, eventually, specific for the place they will occupy. This panels may be performed using a technology that allows to obtain different designs, meeting the different desires of costumers.

Back in 1986, Charles Hull described the additive manufacturing, that includes 3D printing technique, as a process of joining materials to make objects

from 3D model data, layer by layer. [22] Additive manufacturing is a technology that produces 3D tactile physical models, layer by layer, based on Computer-Aided Design (CAD) models. Usually, a Standard Tessellation Language (STL) file (the most commonly used file format for 3D printing) is created and the mesh data is sliced into a build file of 2D layers and sent to the 3D printing machine

Additive manufacturing encompasses several different techniques as: fused deposition modelling (FDM), selective laser sintering (SLS), inkjet 3D printing (3DP), stereolithography (SLA) or even 3D plotting. The selection of the printing technique to be used depends on the starting materials, requirements of processing speed and resolution, costs and performance requirements of the final products. The different techniques are compared in Table 1.4. [23]

Table 1.4 – Additive manufacturing different techniques comparison. [23]

Technique	State of starting material	Typical polymer materials	Working principle	Advantages	Disadvantages
FDM	Filament form	Thermoplastics: PC, ABS, PLA and nylon	Extrusion and Deposition	Low cost, good strength, multi-material capability	Anisotropy, nozzle clogging
SLA	Liquid photo-polymer	Photocurable resin (epoxy or acrylate-based resin)	Laser scanning and UV induced curing	High printing resolution	Material limitation, cytotoxicity, high cost
SLS	Powder	PCL and polyamide powder	Laser scanning and heat induced curing	Good strength, easy removal of support powder	High cost, powdery surface
3DP	Powder	Any materials can be supplied as powder, binder needed	Drop-on-demand binder printing	Low cost, multi-material capability, easy removal of support powder	Clogging of binder jet, binder contamination
3D	Liquid or plotting paste	PCL, PLA, hydrogel	Pressurized syringe extrusion and heat or UV-assisted curing	High printing resolution, soft materials capability	Low mechanical strength, slow

Different materials can be printed and among polymers, thermoplastic polymers are well adequate to be processed by 3D printing. Thermoplastic materials consist of linear or branched chain molecules that have strong intramolecular bonds but weak intermolecular ones, so pure polymer printed objects usually are lack of strength and functionality as fully functional parts. Composites appear to overcome

this problem, because they can combine both matrix and reinforcements properties, achieving better functional and structural performance.

Within this work, FDM technique will be used for the fabrication of the prototype acoustic panels. In FDM, the filament melts into a semi-liquid state at the nozzle and is, then, extruded by the nozzle and layer by layer deposited onto the build platform where layers are fused together and solidified into final parts. The composite materials used in FDM must be in form of a filament to enable the extrusion process. [23] Figure 1.9 is a schematic of FDM. [24]

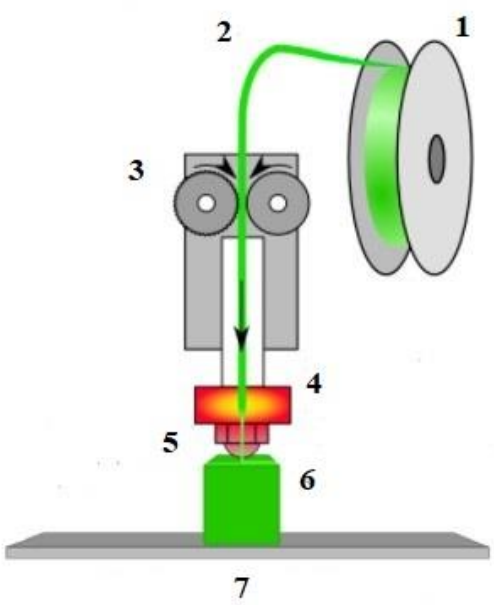

Figure 1.9 - Simplified diagram of the FDM technique: 1- filament spool, 2- filament, 3- extruder, 4- heater block, 5- nozzle, 6- piece and 7- bed. [24]. *The filament is led into the extruder, melting and being extruded into the bed, in the desired x/y/z position.*

The filament in the filament spool (1) is led into the extruder (2) and the extruder uses torque and a pinch system to feed and retract the filament precise amounts (3). In (4), a heater block melts the filament to a useable temperature and the heated filament is forced out the heated nozzle at a smaller diameter (5), being the extruded material laid down on the model where it is needed (6). Finally, in (7), the printing head is moved to the correct x/y/z position for placing the material.

This technique has been widely applied due to its reliability, safety and simple fabrication process, low cost of materials and the availability of a variety of building thermoplastics. [25]

FDM also offers great potential for a range of other materials including metals and composites, as long as the materials can be produced in feedstock filament form of required size, strength and properties. [26]

Besides that, one of the biggest advantages and the main motivation to use additive manufacturing techniques in our project is the fact that this technology allows to produce customized objects with a wide variety of geometries, either simple or complex, for specific applications. [27]

The most commonly used thermoplastics are polycarbonate (PC), acrylonitrile butadiene styrene (ABS) and polylactic acid (PLA), due to their low melting temperature and they are the only thermoplastics with suitable melt viscosity to be used in FDM printers (high enough to provide structural support and low enough to enable extrusion). [23] These thermoplastics are also adequate for industrial applications since they can be easily manipulated in the pre-fusion state at low temperatures, gradually solidifying as they cool down, recovering all their initial properties.

Figure 1.10 presents the processing and life cycle of PLA [28]. PLA is a biopolymer obtained from fungi fermentation of sugars obtained from renewable sources such as sugar cane or corn starch.

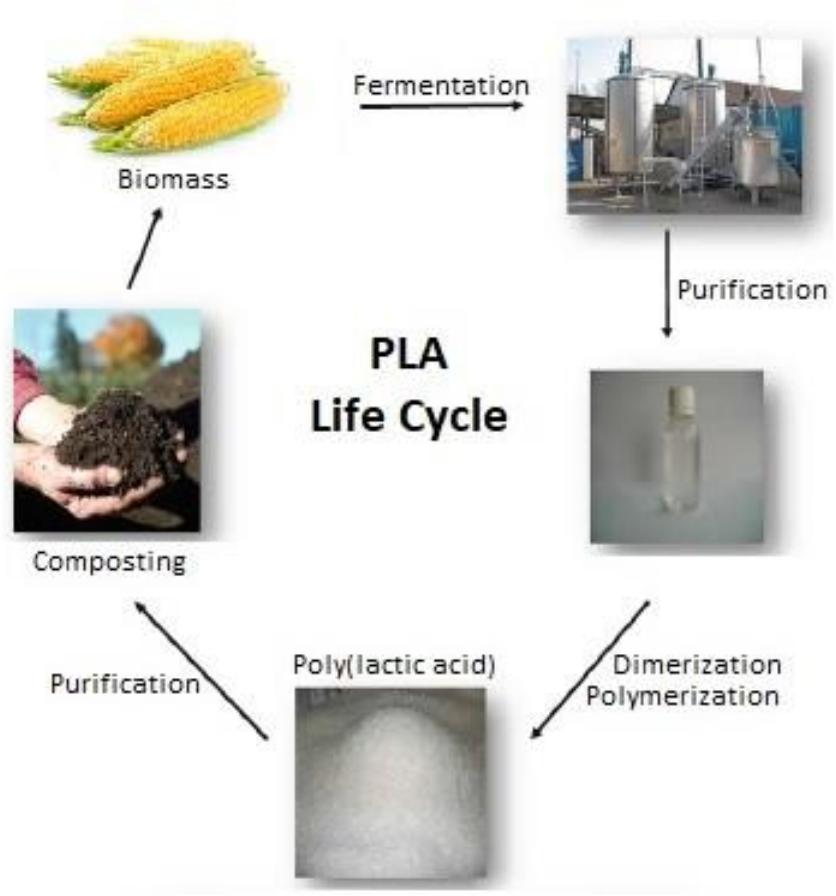

Figure 1.10 – Process and Life cycle of PLA [28].

PLA has melting temperature of 175°C and a glass transition temperature between 55 and 60°C. PLA is fragile, has high stiffness and is well known for its biodegradability and excellent mechanical properties, as Young modulus between 2 and 4 GPa, tensile strength between 50 and 70 MPa and an elongation at break between 2 and 6 % [27]. In addition, PLA has good processability and low production costs. For all these reasons, when compared with polymers like polyethylene (PE), polypropylene (PP) or even polystyrene (PS), PLA is one of the most used polymers. However, it also presents some disadvantages like low thermal resistance and low impact resistance. [29]

Besides that, PLA is also easily combustible and does not meet the safety requirements in many cases leading to a specific need of improvement of the fire resistance performance of this thermoplastic that can be achieved with the usage of flame retardant additives. In spite of the fact that the fire resistance properties of PLA can be improved via introducing flame retardant additives to the PLA matrix, the usage of these additives can cause an increase in the brittleness of the composites, being of extreme importance to find a way to improve both the flame retardancy and toughness of PLA. [29]

Numerous investigations have been carried out aiming to develop composite based filaments for FDM.

Nikzad *et al.* [26] investigated the thermal and mechanical properties of iron/ABS and copper/ABS composites for applications in FDM.

Tian *et al.* [30] proposed a novel 3D printing based fabrication process of Continuous Fiber Reinforced Thermoplastic Composites (CFRTPCs), using a continuous carbon fiber/PLA composite filament. Composite components were fabricated, what demonstrates the process feasibility.

Masood *et al.* [25] developed a new metal/polymer composite for FDM. The material consisted of iron particles in a nylon matrix and was successfully used in FDM for direct rapid tooling of injection moulding inserts.

Drummer *et al.* [31] evaluated the suitability of a PLA and tricalcium phosphate (TCP) composite to be processed by FDM.

Carneiro *et al.* [32] evaluated the potential of polypropylene (PP) and glass-fiber/PP composite as candidates for FDM-based 3D printing technique. It was shown that this technique allows the production of parts with adequate mechanical performance for both materials tested, however, better mechanical properties were achieved with the glass-fiber/PP composite.

Mostly of the composite filaments studies were based on the improvement of the mechanical properties. There is still plenty of room for the development of composite filaments with other functional properties.

1.10. OBJECTIVES

The main goal of this work is the exploitation of rubber based polymeric composites of recycled tires for additive manufacturing, being an acoustic panel, the prototype to be tested.

To meet the challenge, a composite filament containing PLA and recycled rubber must be develop, which encompasses several specific objectives such as:

- Theoretical prediction of the mechanical properties of the composite using Granta Design CES Selector 2017. [33]
- Preparation of a sustainable composite formulation
- Extrusion of filament
- Validation of the filament on the additive manufacturing of a composite panel
- Acoustic characterization of the printed composite panel.

2. EXPERIMENTAL PROCEDURE

2. EXPERIMENTAL PROCEDURE

This chapter describes the different performed tasks of the experimental procedure as well as the characterization techniques used in this work.

The experimental procedure is schematically represented in Scheme 2.1.

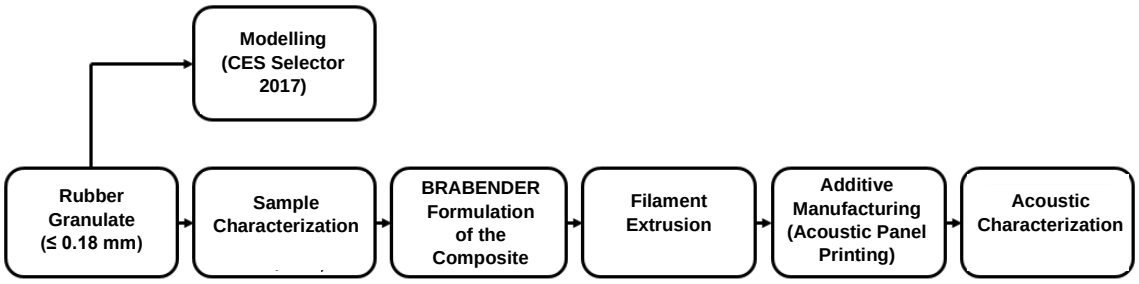

Scheme 2.1 – Schematic representation of the experimental procedure.

2.1. SAMPLE CHARACTERIZATION

2.1.1. SCANNING ELECTRON MICROSCOPY (SEM) AND ENERGY-DISPERSIVE X-RAY SPECTROSCOPY (EDS)

The scanning electron microscopy is a very powerful and versatile technique available for the microstructural characterization. It produces images of a sample by scanning the surface with a focused beam of electrons. From the interaction between the material and the electron beam, a great number of different signals are generated, as shown in Figure 2.1. [34]

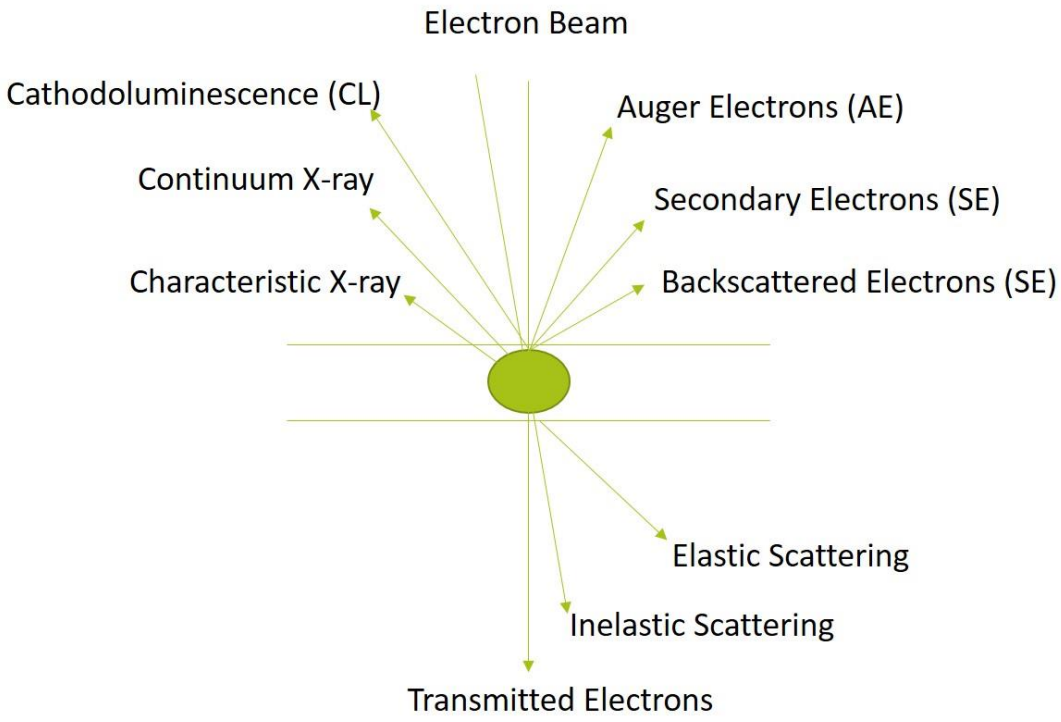

Figure 2.1 - Different signals generated from the interaction between the electron beam and the sample [30].

Each one of these signals can give different kind of information such as crystallography, chemical composition, surface topography, among others. Electron microscopy image can be combined with other characterization techniques to get more information from a specific and localized region of the sample. In fact, energy-dispersive x-ray spectroscopy (EDS) is typically linked with electron microscopy concerning the identification of specific chemical elements in the sample through the analysis of the emitted x-ray radiation. [34]

To prepare the sample for SEM/EDS examination, the materials were fixed using carbon tape to the SEM/EDS sample holder. A carbon coating of the sample was made using an EMITECH K950X, for 5 minutes, with $2x10^{-2}$ mbar vacuum.

For SEM/EDS observations, a HITACHI S-4100 microscope was used, operating with an incident energy of 25 KeV.

2.1.2. FOURIER-TRANSFORM INFRARED SPECTROSCOPY (FTIR)

Fourier Transformed Infrared Spectroscopy (FTIR) consists in the study of the interaction of infrared light with a material. In this technique, infrared radiation passes through the sample and it can be absorbed by the sample or transmitted. The measured signal is accomplished via Fourier transformation (performed by a computer), so that a frequency spectrum can be obtained. The resulting spectrum is unique for each molecule, being a representation the absorption and transmission of this molecule. Each peak of FTIR spectra correspond to the vibrational modes of the atoms constituting the material, being possible to identify qualitatively a material. [35]

A scheme of FTIR apparatus is presented in Figure 2.2.

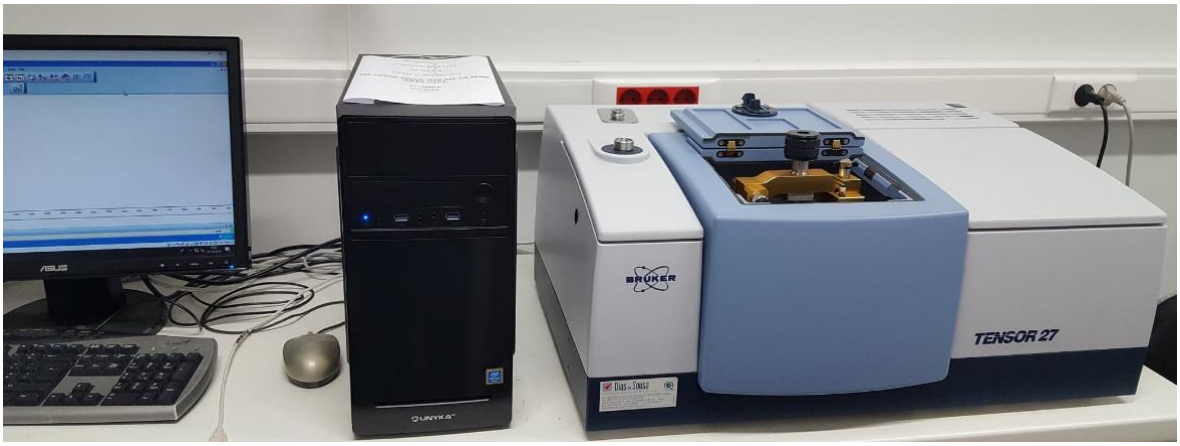

Figure 2.2 – FTIR equipment. In this technique, infrared radiation passes through the sample, being absorbed or transmitted. The measured signal is accomplished by Fourier transformation (performed by a computer) and a frequency spectrum is obtained.

FTIR spectroscopy analyses were performed to identify the functional groups present on the rubber samples.

The FTIR spectra was measured with a Brucker Tensor 27 spectrometer in a spectral range of 4000 to 350 cm^{-1}.

2.1.3. DIFFERENTIAL SCANNING CALORIMETRY/THERMOGRAVIMETRIC ANALYSIS (DSC/TGA)

Differential Scanning Calorimetry (DSC) measures the energy absorbed (endotherm) or produced (exotherm) as a function of time or temperature. It yields peaks related to endothermic and exothermic transitions showing changes in heat capacity and confine quantitative information relating to the enthalpic changes in the polymer. Figure 2.3 presents a DSC graph interpretation of a polymeric material. [36] [37]

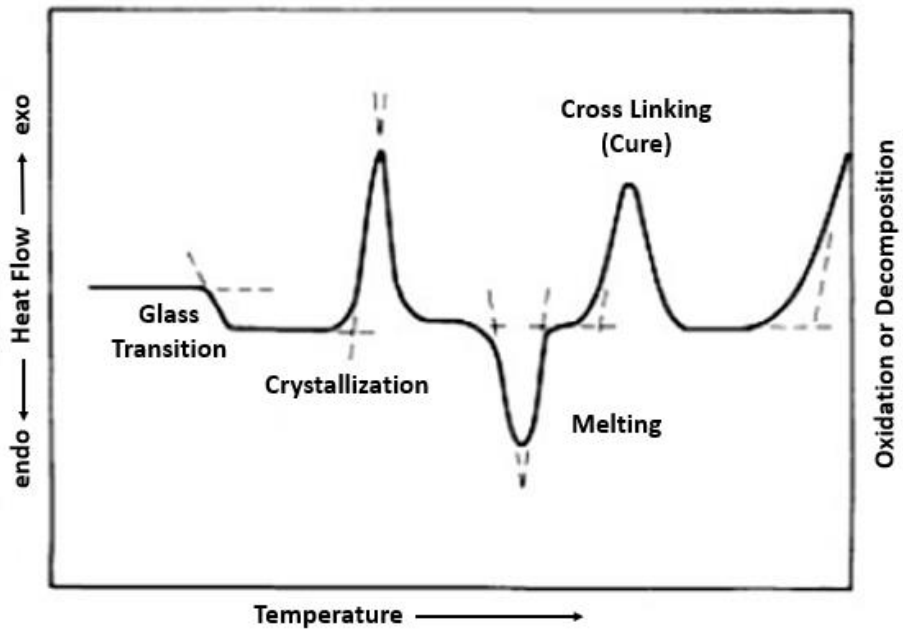

*Figure 2.3 – DSC interpretation of a polymeric material [*36][37]. *DSC measures the energy absorbed or produced as a function of time or temperature and is used to characterize melting, crystallization, curing, loss of solvents and other processes involving an energy change and changes in heat capacity.*

The glass transition temperature, Tg, is an endothermic process. Both amorphous and semicrystalline materials tend to be hard and brittle at temperatures below Tg since the polymer chains are locked in a tangle position, however, surpassing the glass transition temperature, the polymer becomes softer and more ductile since the polymer chains can rotate more easily and slip past each other. [36] [37]

The crystallization temperature (Tc) is an exothermic process that occurs in some polymeric materials. At this temperature there is the formation of intermolecular bonds and the molecules become ordered. [36] [37]

In what concerns melting, it occurs when the material changes from solid to liquid. It is a process that involves energy absorption from the intermolecular bonds, being an endothermic process. [36] [37]

Lastly, the Curing of a polymer occurs when individual chains form strong bonds to other chains (cross linking) and these chains become more ordered. The Curing is an exothermic process. [36] [37]

It is important to notice that different polymers may behave in different ways.

Thermogravimetric Analysis (TGA) measures the mass changes of a sample as a function of the temperature what which the sample is exposed for a period, being possible to monitor physical and chemical changes of the sample. There are several effects that may lead to mass changes, gain or loss, as for example: decomposition of organic substances, thermal decomposition, evaporation of volatile constituents, breaking of chemical bonds, between others. [38]

The equipment used was a Setaram Setsys Evolution 1750, in TG-DSC mode (type S). The test was conducted in a nitrogen atmosphere from 25 to 500°C, with a heating rate of 10°C/min.

2.2. FORMULATION OF THE COMPOSITE

In this task, the formulation of the composite is performed using a Brabender mixer (Figure 2.4), kindly borrowed by Professor Victor Neto from the Department of Mechanical Engineering of the University of Aveiro. The raw material is loaded through the top opening into the previously heated mixer bowl where it is homogenized by specially shaped mixing blades. If it is connected to a drive unit (torque rheometer), the torque and the stock temperature can be measured and recorded during the mixing process. This torque mirrors the resistance the material opposes to the rotating blades during the mixing process. The corresponding torque

moves a dynamometer out of its zero position. For each sample material, a torque and stock temperature versus time can be recorded. [39]

Figure 2.4 - Brabender mixer equipment [39]. *In this equipment, the raw material is homogenized by specially shaped mixing blades, in the previously heated mixer bowl.*

In the mixture PLA pellets from 3devo company and the rubber granulate with size of ≤ 0.18 mm were used. Glycerol from BDH with a purity of 99.5% was used as a plasticizer.

The several different tests, presented in Table 2.1, were performed aiming at the selection of the optimal experimental mixing conditions.

Table 2.1 - Different mixture compositions and parameters tested in the BRABENDER mixer. Mixtures of PLA and rubber were prepared, with rubber percentages, in mass, between 10 and 60%. A rubber percentage of 20 wt.% was also tested with the addition of glycerol as a plasticizer.

Rubber (wt.%)	Additive	Total Mass (g)	Temperature (°C)	Rotation (rpm)	Time (min)
10	-	20	190	70/90	12
30	-	20			
60	-	20			
10	-	30			
20	-	30			
30	-	30			
40	-	30			
60	-	30			
20	2% Glycerol	30			

The mixture was performed for 12 min at a temperature of 190°C. In the first step, half of the quantity of PLA was added with a blend rotation of 70 rpm, until PLA's melting. After, in a second step, the rubber was added to the mixture with a blend rotation of 90 rpm and, finally, the rest of the PLA was added to the mixture.

2.3. FILAMENT EXTRUSION OF THE COMPOSITE

A 3devo NEXT Extruder, shown in Figure 2.5, was used to extrude into a filament form the different composite compositions.

The customization of the material profile was done in the control panel where the extrusion conditions were selected, and the hopper was filled with our composite mixture. The mixture was pushed through 4 heating zones by a nitride hardened steel extruder screw. The filament was guided into the positioner and locked in the spool winder to coil the filament. [40]

Figure 2.5 - 3devo NEXT Extruder [35]. This equipment was used to extrude into a filament form the different composite compositions.

The extrusion conditions were carefully selected using typical literature conditions of filament extrusion, considering the matrix polymer and adjusted according to the experimental observations.

The 4 heating zones were defined as $T_1 = 150°C$, $T_2 = 180°C$, $T_3 = 185°C$ and $T_4 = 170°C$, the extruder screw rotation set at 5 rpm and fan speed at 22%, as represented in Figure 2.6.

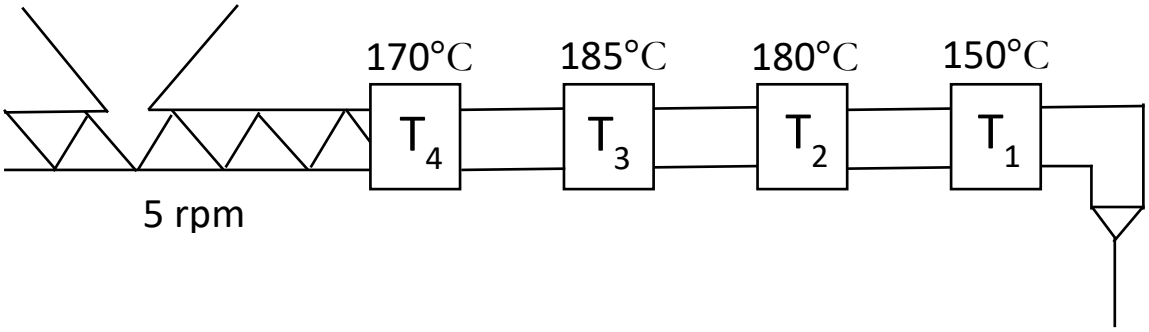

Figure 2.6 – Scheme of the extrusion process. The mixture was pushed through 4 heating zones (T_4, T_3, T_2 and T_1) by a nitride hardened steel extruder screw, operating at 5 rpm.

The extrusion of only PLA pellets was firstly performed to make sure that the extruder was totally clean and ready for the extrusion of our mixture. After that, the extrusion of our mixtures was performed, and, in the end, a new pure PLA extrusion was performed. The filaments used for the additive manufacturing and its characteristics are presented in Table 2.2.

Table 2.2 - Naming of the filaments used in the additive manufacturing.

Filament name	Characteristics
F1	Filament with 20 wt.% rubber + 2 wt.% glycerol and a mean diameter value of 1.17 mm (Figure 3.7 e)
F2	Filament with 20 wt.% rubber + 2 wt.% glycerol and a mean diameter value of 1.97 mm (Figure 3.9)

It is still important to say that filament F1 was locked and coiled in the spool winder of the extruder (spooling on), while filament F2 was coiled manually (spooling off).

2.4. ADDITIVE MANUFACTURING

SolidWorks software [41] was used to design an acoustic panel, following the design of a commercial panel. A popular design of sound absorption panels is the "egg box type" and this was the design type that we have tried to follow.

For the printing of the panels, the Fused Filament Fabrication (FFF) technique was used in an Anet A8-B 3D Printer, as shown in Figure 2.7.

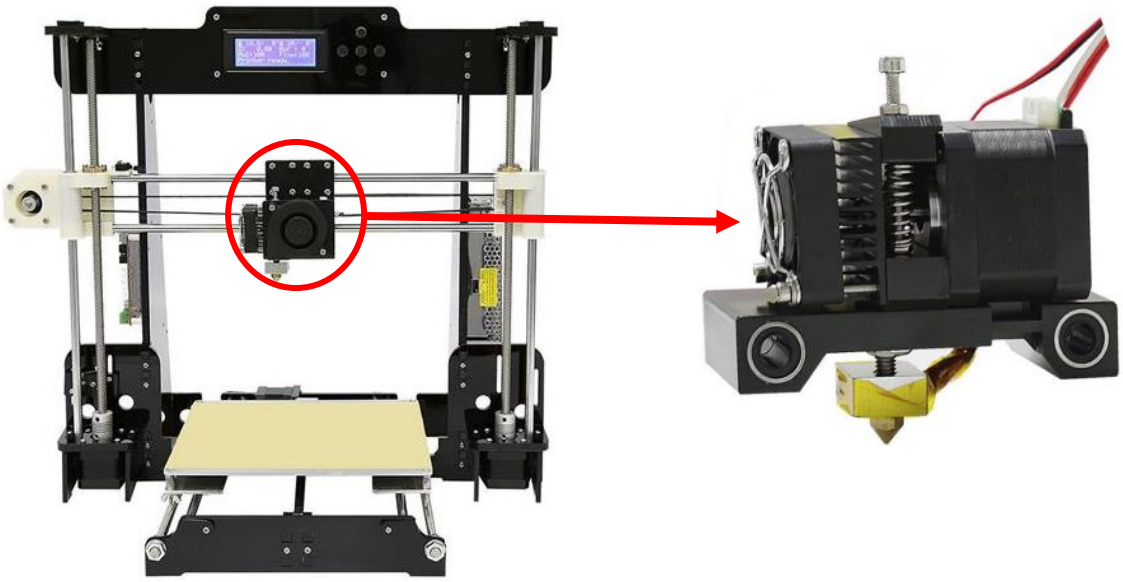

Figure 2.7 - Anet A8-B 3D Printer (left); Extruder nozzle ampliation (right) [50].

The first printing attempts were a $8\ cm^3$ cube, where the printing parameters were selected according to the experimental observations. Several temperatures and nozzle diameters were tested, to improve the printing. According to this, the temperature selected was T = 170°C and the nozzle selected was the $0.6\ mm$ diameter one. The $8\ cm^3$ cube was printed with filament F1.

An attempt of printing the "egg box type" panel was also performed, however with filament F2, with a nozzle diameter of 0.6 mm and an extrusion temperature of

T = 170°C. The panel was designed with a quadrangular base of 5 cm side, with four quadrangular pyramids of 1 cm height on the top.

Finally, to perform the acoustic characterization, 3 round samples with a diameter of 5 cm and 3 cm of height were printed. Sample A1 (a flat PLA sample), sample A2 (a flat sample printed with filament F2) and sample A3 (an "egg box type" sample printed with filament F2). The characteristics of the printed samples are described in Table 2.3.

Table 2.3 – Naming and characteristics of the round printed samples.

Sample	Characteristics
A1	Flat PLA sample
A2	Flat sample printed with filament F2
A3	"Egg box type" sample printed with filament F2

Before the acoustic characterization of the samples, their density was determined by the Archimedes method.

2.5. DENSITY DETERMINATION

The density of the samples A1 and A2 were determined by the Archimedes' Principle that states that an object immersed in a fluid is buoyed up by a force equal to the weight of the fluid that it displaces [42]. In the measurements performed, our samples were immersed in water.

To determine the density of the samples, the following equation is used (Equation 2.1):

$$\rho_s = \frac{m_s}{m_s - m_i} \times \rho_w \qquad \text{(Equation 2.1)}$$

Where ρ_s is the density of the sample, m_s the mass of the sample, m_i the mass of the immersed sample, and, ρ_w, the water density.

For performing the Archimedes' Principle, an AND Electronic Balance FA-2000 was used. The samples were previously weighted. A schematic representation

of the experimental procedure adopted to determine both samples' density is presented in Figure 2.8.

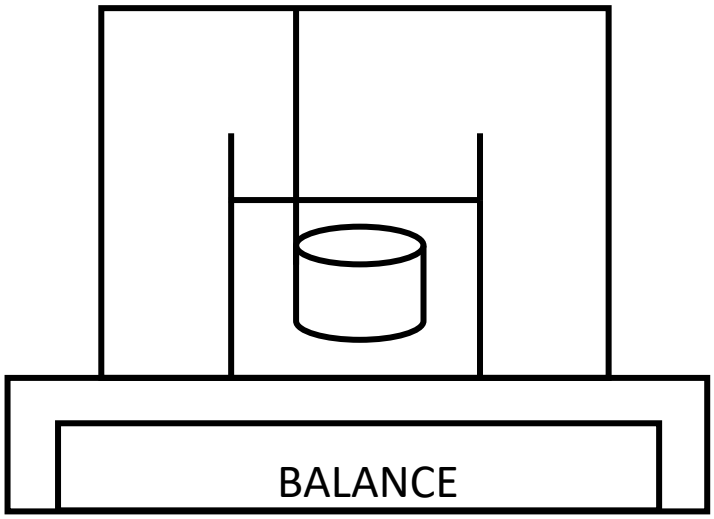

Figure 2.8 – Schematic representation of the Archimedes' Principle performed to determine the density of both samples A1 and A2.

2.6. ACOUSTIC CHARACTERIZATION

Using a wave impedance tube, we can determine the acoustic characteristics of a material. This method is one of the most important techniques in the acoustic materials characterization and the device used for measuring the sound absorption coefficient is shown in Figure 2.9. [43]

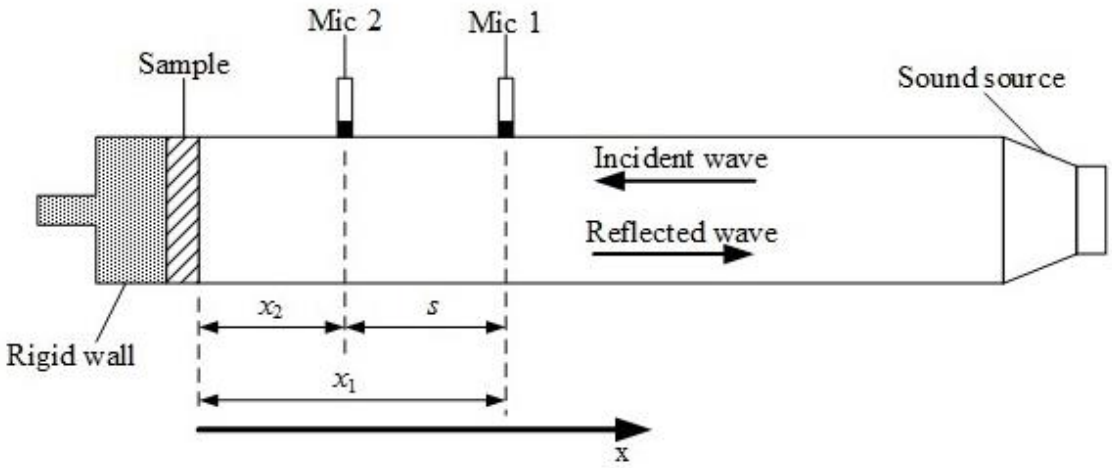

Figure 2.9 - Scheme of the standard test method for Impedance and Absorption of Acoustical Materials [43].

In the sound source, a plane wave is generated and propagated through the impedance tube, until its collision with the sample. The wave is then reflected. With the amplitude of both waves we can calculate the reflection coefficient (Equation 1.1) and, consequently, the absorption coefficient (Equation 1.2).

The efficiency of a material in absorbing acoustical energy at a specified frequency is given by its absorption coefficient at that frequency. This quantity is the fractional part of the energy of an incident sound wave that is absorbed (not reflected) by the material. Thus, if sound waves strike a material, and if 55 % of the incident acoustical energy is absorbed and 45 % is reflected, the absorption coefficient of the material is 0.55. [21]

To perform this task, an impedance tube, two microphones and a digital frequency analysis system for the determination of normal incidence sound absorption coefficients and normal specific acoustic impedance ratios of materials were used. The characterization took place in the Department of Civil Engineering, in the University of Coimbra, and was performed according to the ASTM E1050 and by Professor Luis Godinho. [43]

The microphones were G.R.A.S. 46E from G.R.A.S SOUND & VIBRATION, represented in Figure 2.10.

Figure 2.10 – G.R.A.S. 46E microfones.

The device used to generate the plane wave was a NI USB 4431, represented in Figure 2.11.

Figure 2.11 – NI USB 4431 device.

The impedance tube section should be round or rectangular, smooth, non-porous and absent of all kind of wastes. A round section was selected in this work. The dimensions of the impedance tube section have influence in the range of frequencies analysis. The upper working frequency, Fu, relates directly with the diameter of the impedance tube section, as shown in Equation 2.2.

$$Fu = \frac{K \times c}{\emptyset} \qquad (Equation\ 2.2)$$

Where, K is a constant with a value of 0.586, c is the speed of sound in the tube in m/s and Ø, the diameter of the tube in m.

The lower working frequency, Fl, is function of the space between microphones, which expression is shown in Equation 2.3.

$$Fl >> 0.01 \times \frac{c}{s} \qquad (Equation\ 2.3)$$

The spacing between microphones, s, for determination of the lower working frequency is also a function of the upper working frequency, Fu, as shown in Equation 2.4.

$$s < 0.8 \times \frac{c}{2 \times Fu} \qquad (Equation\ 2.4)$$

The diameter of the impedance tube section used was 5 cm and so, the upper working frequency, Fu, was determined using Equation 2.2.

$$Fu = \frac{0.586 \times 340}{0.05} = 3984.8\ Hz$$

The following step consisted in the calculation of the spacing between microphones through the application of Equation 2.4.

$$s = 0.8 \times \frac{340}{2 \times 3984.8} = 0.034\ m$$

After determining the spacing between microphones, is now possible to determine the lower working frequency, Fl, through the application of Equation 2.3.

$$Fl \geq 0.01 \times \frac{340}{0.034} \geq 100\ Hz$$

The setup for the acoustic characterization is represented in Figure 2.12.

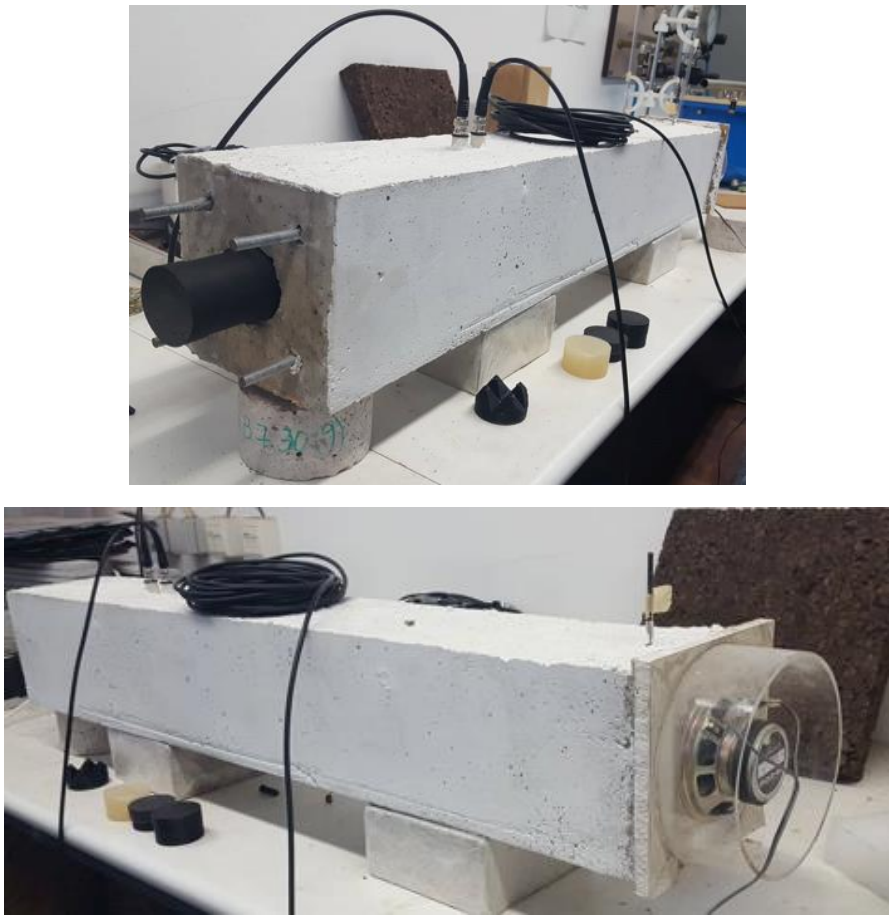

Figure 2.12 – Setup of the wave impedance tube.

3. RESULTS AND DISCUSSION

3. RESULTS AND DISCUSSION

This chapter presents and discusses the results obtained in this work. As a starting point the results of the theoretical prediction of the properties of composites of PLA and rubber, supported by the Granta Design CES Selector 2017, will be presented and their analysis related with the next experimental steps. In the second subchapter, the received recycled tire granulates from RECIPNEU, will be characterized in order to get the knowledge on the raw materials to be able to optimize the composites under study. The third subchapter describes the optimization of the composite formulation and filament preparation and explains the printing process. After all these steps and, as part of the fourth subchapter, the evaluation of the main properties of the composites is presented and discussed, with a special focus on the acoustic behavior and density of the composites.

3.1. THEORETICAL PREDICTION OF THE COMPOSITES BEHAVIOUR

In this task, a Granta Design software called CES Selector is used to select the composition of the composite based on the prediction of properties variation with the content of filler in this case as a function of the rubber granulate to be included. [44] This software is composed by several different tools, being the Synthesizer Tool the main one for our work. Synthesizer Tool allows the performance prediction of composite materials in different geometries.

In our work, a composite simple bound (particulate) model was chosen, assuming a continuous matrix (PLA) and a filling material (SBR), and 6 records were generated with a particulate volume fraction ranging from 1 to 70 %. Notice that, in this work, PLA was chosen as the continuous matrix since it is a biopolymer (made from renewable sources), environmentally friendly, that has great thermal processability, being possible to process by extrusion, and is one of the most used polymers in additive manufacturing. [45]

The theoretical behavior of the composite's mechanical properties (tensile strength, yield strength, compressive strength and Young modulus) and density was predicted and is represented in Figure 3.1.

In Figure 3.1 a), a graph of the theoretical prediction of the tensile strength of the composite as a function of the volume percentage of rubber to be included is plotted. For a particle volume fraction of 1 %, a tensile strength of around 5 MPa was registered, however, a huge drop of the tensile strength was registered, and for a particle volume fraction of 10 %, a tensile strength of around 0.5 MPa was recorded. Increasing the particle volume fraction until 70 %, the value of the tensile strength was almost constant below 0.5 MPa.

In Figure 3.1 b), a graph of theoretical prediction of the yield strength of the composite as a function of the volume percentage of rubber to be included is plotted. For a particle volume fraction of 1 %, the value of yield strength registered was around 6 MPa. As the particle volume fraction is increased, the yield strength of the composite suffers a huge drop, being registered a yield strength of around 0.5 MPa for particle volume fraction of 10 % and even lower values of yield strength for higher particle volume fractions.

In Figure 3.1 c), a graph of theoretical prediction of the Young Modulus of the composite as a function of the volume percentage of rubber to be included is plotted. For a particle volume fraction of 1 %, the value of the Young Modulus is around 0.35 GPa. As the particle volume fraction is increased, lower values of Young Modulus are registered as, for example, a Young Modulus of around 0.025 GPa for a 10 % particle volume fraction and even lower values until a 70 % particle volume fraction.

In Figure 3.1 d), a graph of theoretical density of the composite as a function of the volume percentage of rubber to be included is plotted. For a particle volume fraction of 1 %, a density of 1225 kg/m^3 is registered. This density stays almost constant until around a particle volume fraction of 20 %, where the density of the composite suffers a huge drop, being recorded a density of around 950 kg/m^3 for a particle volume fraction of 27 %. After this, the density of the composite increases and, for a particle volume fraction of 70 %, a density of around 1075 kg/m^3 is recorded.

In Figure 3.1 e), a graph of theoretical prediction of the compressive strength of the composite as a function of the volume fraction of the volume percentage of rubber to be included is plotted. For a particle volume fraction of 1 %, the value of

the compressive strength is 7 MPa. Increasing the particle volume fraction to 10 %, the value of the compressive strength drops for around 0.7 MPa, staying this value almost constant for higher particle volume fractions.

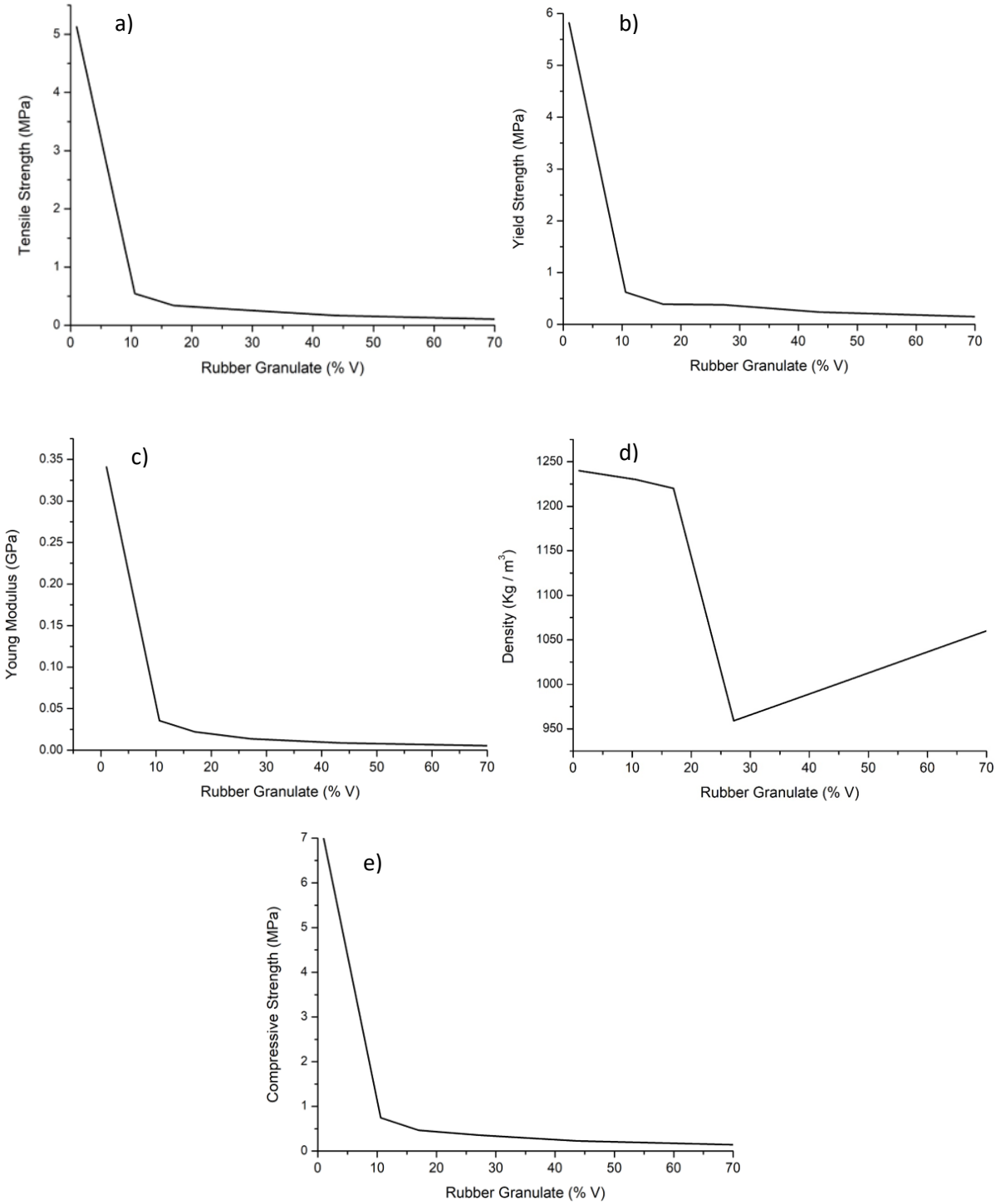

Figure 3.1 – Theoretical prediction of the composites behavior: a) tensile strength, b) yield strength, c) Young modulus, d) density and e) compressive strength, as function of the rubber granulate (% V). The mechanical properties of the PLA matrix decreased with the rubber addition, reaching a minimum for 10 % in volume, being almost constant higher percentages. The composites' density was constant until around 20 % in volume, perceiving a substantial decrease between 20 and 30 % in volume, evidencing a slight increase of this value for increasingly high rubber percentages.

The theoretical prediction of the composites behaviour demonstrated that the mechanical properties (tensile strength, yield strength, compressive strength and Young modulus) of the PLA matrix decrease with the filler addition, rubber, being the variation more accentuated for low percentages of the filler, reaching a minimum value for around 10 % in volume, being almost constant after this value. Concerning the composites' density, the theoretical prediction pointed to a constant density value until around 20 % in volume, perceiving a substantial decrease between 20 and 30 % in volume and, afterwards, a density stability for higher percentages of rubber, evidencing a slight increase of this value for increasingly high rubber percentages. For these reasons, 20 % mass fraction of granulate was selected for our further studies.

3.2. RAW MATERIAL CHARACTERIZATION

Within this partnership, RECIPNEU, supplied 8 different types of granulates designated as: DC-8000, DC-3080, DC-1430, DC-1014, DC-0814, DC-0725, DC-0308 and DC-FLEXYGRAN. Their specifications are presented in Table 3.1.

Table 3.1 – Specifications of the different types of granulates provided by RECIPNEU. [13] *DC-8000 sample was selected because of its lower nominal dimensions.*

Reference	Mesh	Nominal Dimensions (mm)
DC-8000	#80	≤ 0.18
DC-3080	#30 - #80	0.18 – 0.60
DC-1430	#14 - #30	0.60 – 1.40
DC-1014	#10 - #14	1.40 – 2.00
DC-0814	#08 - #14	1.00 – 2.40
D C-0725	#07 - #25	0.80 – 2.50
DC-0308	#03 – #08	2.40 – 6.30
DC-FLEXYGRAN	≥ #03	≥ 6.30

DC-8000 sample was selected because of its lower nominal dimensions that could be an advantage in the optimization of the composite formulation.

The composition of the cryogenic rubber granulates was also supplied by RECIPNEU and is presented in Table 3.2.

Table 3.2 – RECIPNEU's information about the composition of the cryogenic rubber granulates [10].

Component	Concentration (wt.%)
Vulcanized SBR	52.1
Vulcanized NR	
Other vulcanized rubbers	
Carbon Black	27.2
Silica	6.3
Aromatic Oil	7.3
Zinc Oxide	2.0
Sulfur	1.7
Stearic Acid	1.2
Antidegradants	2.0

The materials characterization was performed by means of 3 different techniques: SEM/EDS, FTIR and DSC/TGA.

3.2.1. SCANNING ELECTRON MICROSCOPY (SEM) AND ENERGY-DISPERSIVE X-RAY SPECTROSCOPY (EDS)

The microstructure of the DC-8000 sample was determined by SEM, and the elemental composition was determined by EDS.

Figure 3.2 shows the SEM micrographs of the DC-8000 and, Figure 3.3, the correlated EDS analysis.

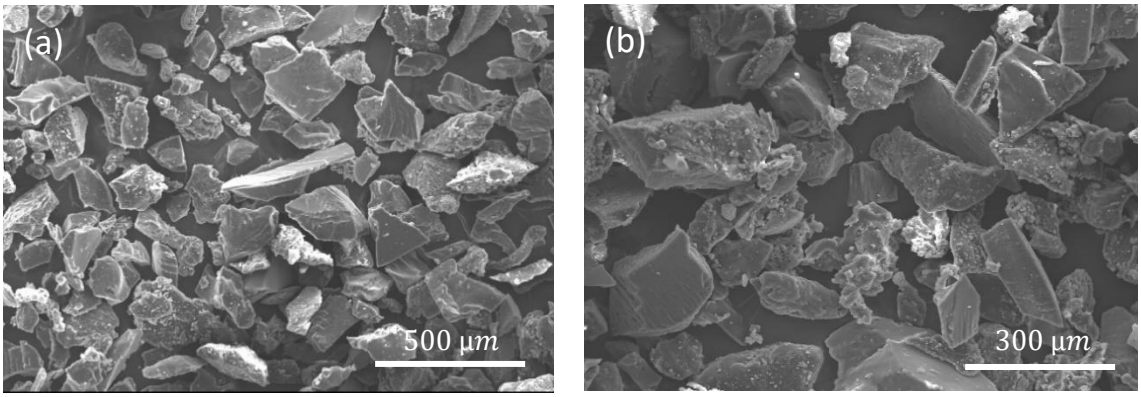

Figure 3.2 - SEM micrographs of DC-8000. The grains obtained present irregular rectangular shapes, a flat morphology, and a relative smooth surface, typical characteristics.

As it was expected, the grains observed in Figure 3.2 present irregular rectangular shapes, a flat morphology and a relative smooth surface, typical characteristics of cryogenic rubber granulates. The correspondent EDS spectra is presented in Figure 3.3.

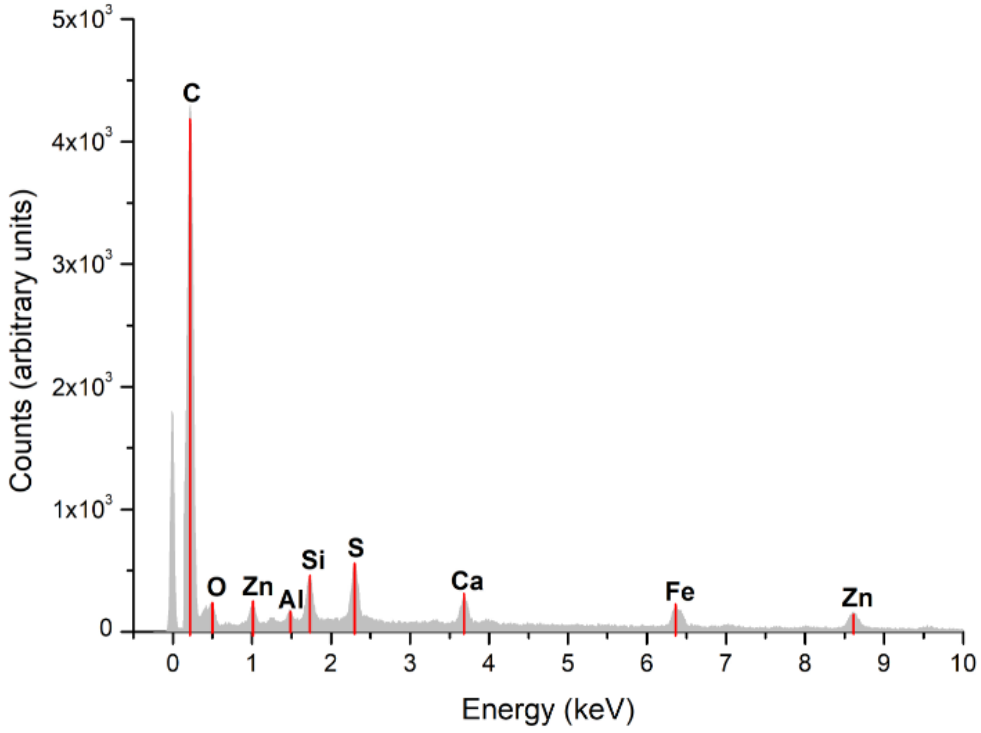

Figure 3.3 – EDS analysis of DC-8000 sample. Carbon, sulfur, silica, zinc, oxygen, calcium, aluminum and iron were identified as the main components of these rubber granulates.

EDS spectra presented in Figure 3.3 identify as the main components of these rubber granulates carbon, sulfur, silica, zinc, oxygen, calcium, aluminum and

iron. This is an expected result and supports the data previously presented (Table 3.2) and supplied by the company.

As indicated in Table 3.2, the cryogenic rubber granulates used in this work are mostly composed by styrene - butadiene rubber (SBR), natural rubber (NR) (Polyisoprene) and other types of rubber, all vulcanized. Carbon black and silica are also present in the composition, as well, working as reinforcing fillers. Also, aromatic oils, zinc oxide, sulfur, stearic acid and antidegradants are present in the composition. The role of aromatic oils is to facilitate the processing of the rubber compounds, being also an essential component for the technical performance of the tires. Zinc oxide and stearic acid, together, will react with sulfur and produce a strong vulcanizing agent, while the zinc oxide will induce the breaking of the sulfur molecule, forming new crosslinking bonds, stabilizing the vulcanization network and improving the aging resistance. Also, calcium and aluminum are present, in small amounts, working as facilitators during the different stages of tire production. [2]

3.2.2. FOURIER-TRANSFORM INFRARED SPECTROSCOPY (FTIR)

The FTIR spectroscopy analyses were performed to verify qualitatively the functional groups present on the rubber samples and to provide new data about the cryogenic rubber particles to RECIPNEU. It is expected to detect the vibrations corresponding to the functional groups present in the tires such the ones assigned to the rubber (CH_2 and CH_3 bonds) and functional groups related with the rubber vulcanization. The FTIR spectrum is represented in Figure 3.4.

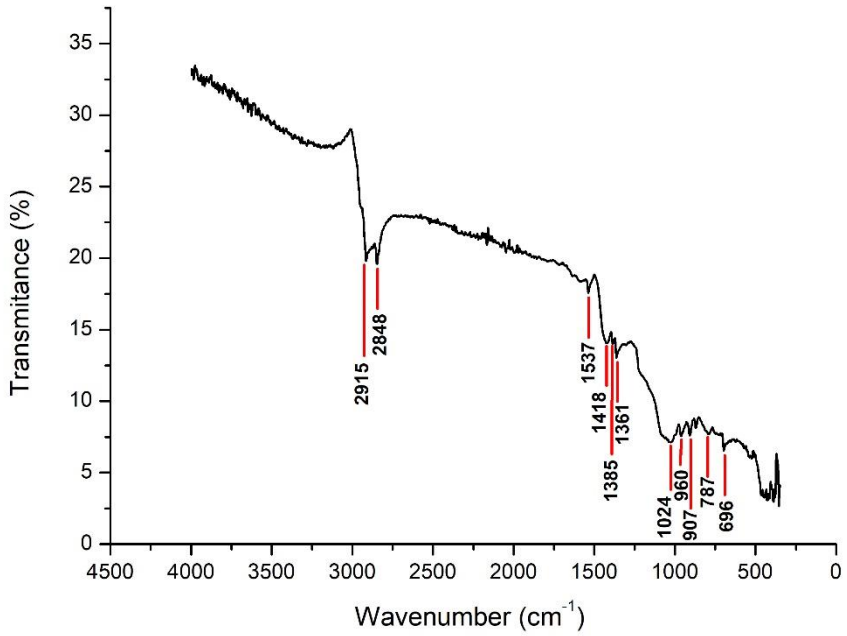

Figure 3.4 – Rubber sample (DC-8000) FTIR analysis. The vibrations detected correspond to the functional groups present in the tires such the ones assigned to the rubber and functional groups related with rubber vulcanization.

The bands at 696 and 787 cm^{-1} are ascribed to the out of plane bending vibrations of aromatic ═C─H and C═C groups of polystyrene in SBR and the bands at 1024 and 907 cm^{-1} attributed to the out of plane bending vibrations of C─H of vinyl groups and the band at 960 cm^{-1} attributed to the trans ─CH═CH─ group vibrations of butadiene presented in SBR. The peaks in the region of 2915 and 2848 cm^{-1}, as well as the peaks at 1418 and 1385 cm^{-1}, are assigned to the $-CH_3$ and $-CH_2$ bonds, relative to the rubber structure. The band at 1361 cm^{-1} attributed to the anti-stretch S═O and, the band at 1537 cm^{-1}, attributed to the anti-stretch C═S. [46] [47]

3.2.3. DIFFERENTIAL SCANNING CALORIMETRY/THERMOGRAVIMETRIC ANALYSIS (DSC/TGA)

More new data is provided to RECIPNEU, analyzing the DSC/TGA results of the cryogenic rubber particles (DC-8000). The DSC was performed in order to understand and characterize the processes occurring in the RECIPNEU cryogenic rubber granulates when an energy change is involved. Also, the mass of the sample was monitored as function of the temperature, by TGA. The thermal analysis of the used cryogenic rubber granulates (DC-8000) is represented in Figure 3.5.

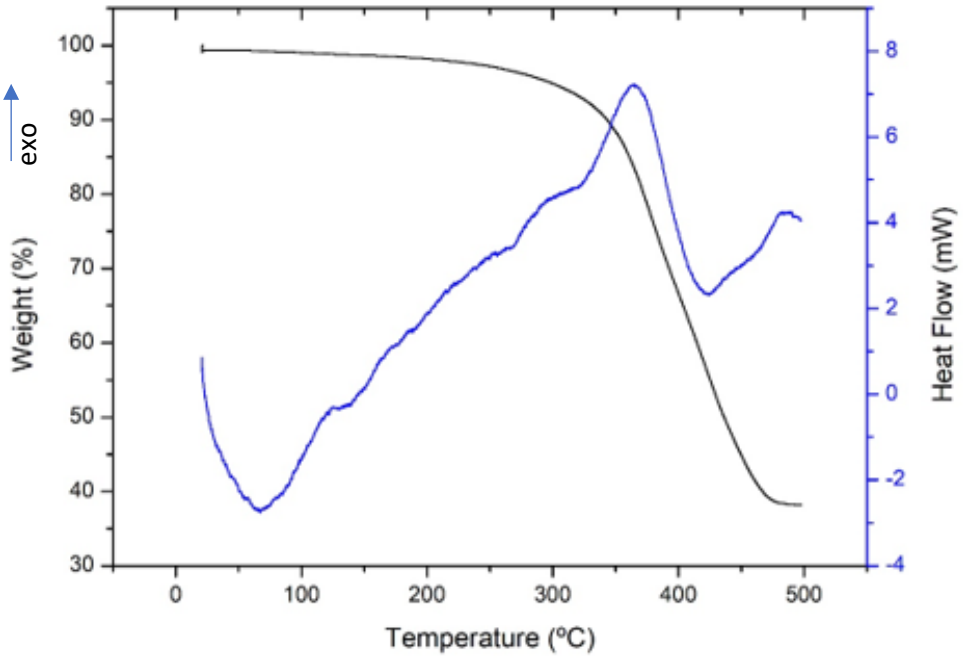

Figure 3.5 – DSC/TG analysis of the cryogenic rubber granulates (DC-8000). The recycled tires granulate is almost stable until 300 °C. Above 300 °C and up to 500 °C a huge drop of mass around 60 % is visible. At 365 °C is visible an exothermic peak related with the initiation of the decomposition of the rubber granulates. At 420 °C, there is an endothermic peak considered to be caused by partial oxidation of carbon black.

Upon heating, the recycled tires granulate is almost stable up to 300 °C. The weight loss is almost negligible, being evident the hydrophobic nature of the sample characterized by the absence of residual water. Only above 300 °C and up to 500 °C, a huge drop of the granulate mass of around 60 % is visible. This weight loss may be associated to the cleavage of the sulfur bonds with consequent combustion [48] of the organic groups of the polymeric part of the rubber. The remaining 40 %, in good agreement with the composition of the granulates (Table 3.2) should be

related with the black carbon, silica, sulfur and metallic species contained in the recycled tires granulates.

Corroborating the observations of the weight loss during the heating, the DTA curve presents at 365 °C an exothermic peak that is related with initiation of the decomposition of the rubber granulates and associated to the cleavage of the sulfur bonds with consequent combustion of the organic groups of the polymeric part of the rubber and, as described above, associated with an accentuated weight loss.

At a temperature around 420 °C, there is an endothermic peak considered to be caused by partial oxidation of carbon black. [48]

3.3. PREPARATION OF THE COMPOSITE FORMULATION

Based on the theoretical prediction of the composites behaviour, mixtures of PLA and rubber were prepared, with rubber percentages, in mass, between 10 and 60 % (Table 2.1).

Our theoretical calculations show that the properties of PLA are considerably affected by the presence of the rubber fillers and this variation is accentuated up to 10 % in volume of rubber and after that the variation of the calculated mechanical properties is almost unnoticeable. In addition, the theoretical density of the composites, starts to be affected only after 20 % in volume. For these reasons, 20 % mass fraction of granulate was selected for our further studies.

Initially, PLA and rubber granulate mixtures with a total mass of 20 g were performed, however, this quantity was not enough to ensure the good mixing of the components, since some parts of the mixture were only rotating around the blades, not really mixing. Then, the value of the total mass was increased to 30 g (maximum supported by the used Brabender mixer) and an ideal mixture between the different components was achieved since, by experimental observation, all mixture components were connected and correctly mixing. As a reminder, the formulations prepared for testing on the filament extrusion were the ones presented next in Table 3.3.

Table 3.3 - Different mixture compositions and parameters tested in the BRABENDER mixer. Mixtures of PLA and rubber were prepared, with rubber percentages, in mass, between 10 and 60%. A rubber percentage of 20 wt.% was also tested with the addition of glycerol as a plasticizer.

Rubber (wt.%)	Additive (wt.%)	Total Mass (g)	Temperature (°C)	Rotation (rpm)	Time (min)
10	-	30	190	70/90	12
20	-	30			
30	-	30			
40	-	30			
60	-	30			
20	2% Glycerol	30			

Several different rubber percentages were tested (10, 20, 30, 40 and 60 wt.%) without any additive. A rubber percentage of 20 wt.% was also tested with glycerol as additive.

Glycerol, that is a colorless, odorless, viscous liquid, is very effective working as a plasticizer and lubricant, being also used to impart flexibility [49], reasons why it was chosen to improve the mixtures of PLA and rubber and, consequently, the produced filaments.

The obtained composite granulates, are shown in Figure 3.6

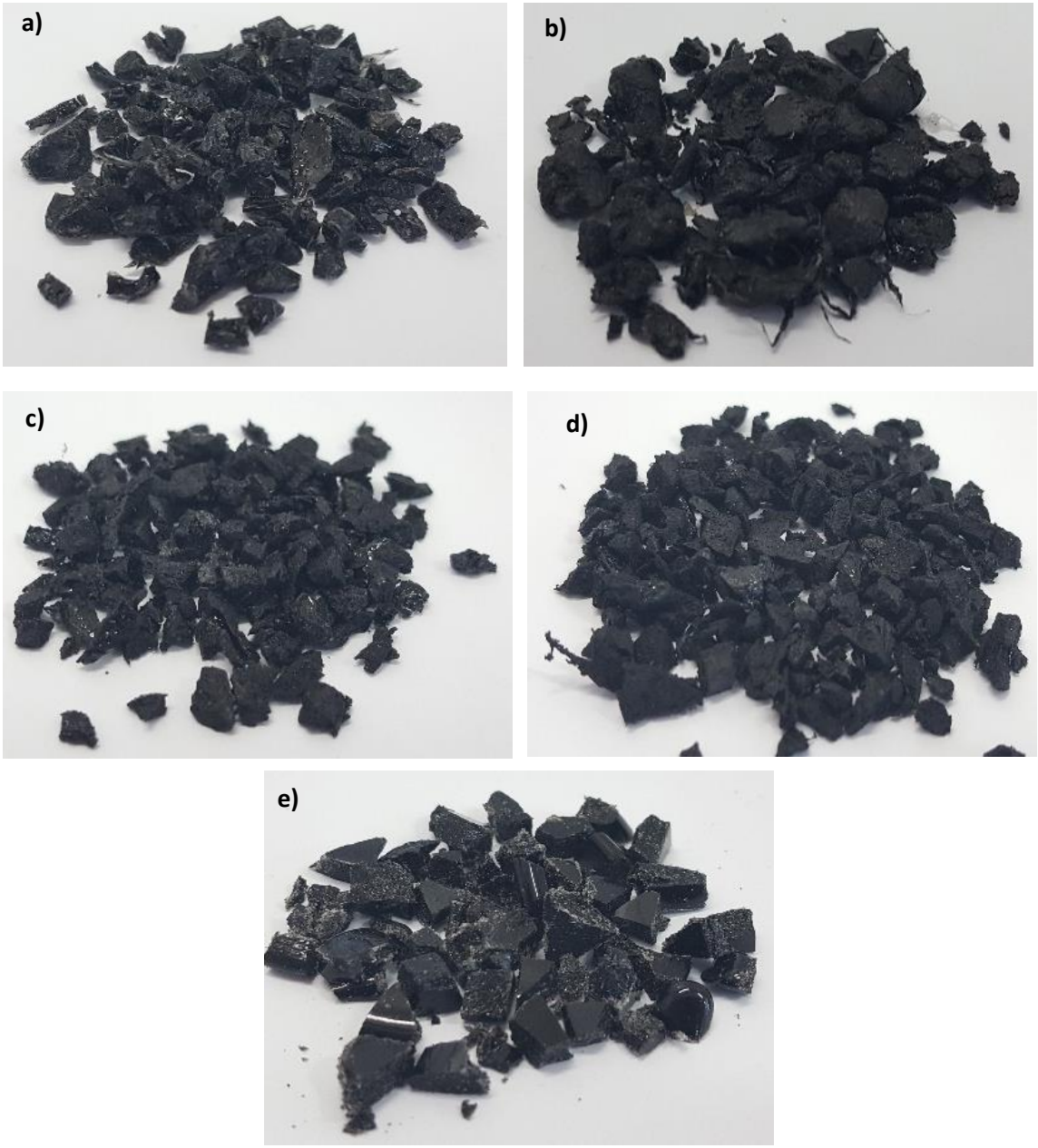

Figure 3.6 – Different composite mixtures tested: a) 10 wt.% rubber; b) 20 wt.% rubber; c) 40 wt.% rubber; d) 60 wt.% rubber; e) 20 wt.% rubber + 2 wt.% glycerol. The highest rubber percentages tested (40 and 60 wt.%) were brittle, while the lowest rubber percentages tested (10 and 20 wt.%) were stiff). Mixture 20 wt.% rubber + 2 wt.% glycerol turned liquid but presented a fast solidification.

For the highest rubber percentages tested (40 and 60 wt.%), it was evident the brittleness of the formulations, once both were breaking easily. On the opposite, for the lowest rubber percentages tested (10 and 20 wt.%), the mixture obtained was stiff. Both these observations are well in accordance with the theoretical prediction of the composites behavior performed, since that for higher rubber percentages, the mechanical properties of the composites obtained were lower.

Mixture 20 wt.% rubber + 2 wt.% glycerol turned liquid, however it showed a very fast solidification (matter of seconds) and a “glass-type” surface. In Table 3.4, the experimental observations are registered.

Table 3.4 - Experimental observations of the different composite formulations tested.

Rubber (wt.%)	Observation
10	Stiff mixtures, extremely hard to break into smaller pieces
20	
40	Brittle mixtures, easily breaking; Increasing the rubber percentage, we increase the mixture brittleness
60	
20 + 2% glycerol	Liquid mixture, with a very fast solidification (seconds); “glass-type” surface;

3.4. FILAMENT EXTRUSION AND CHARACTERIZATION

The different composite mixtures were then tested to be extruded in filament form and the results are represented in Figure 3.7.

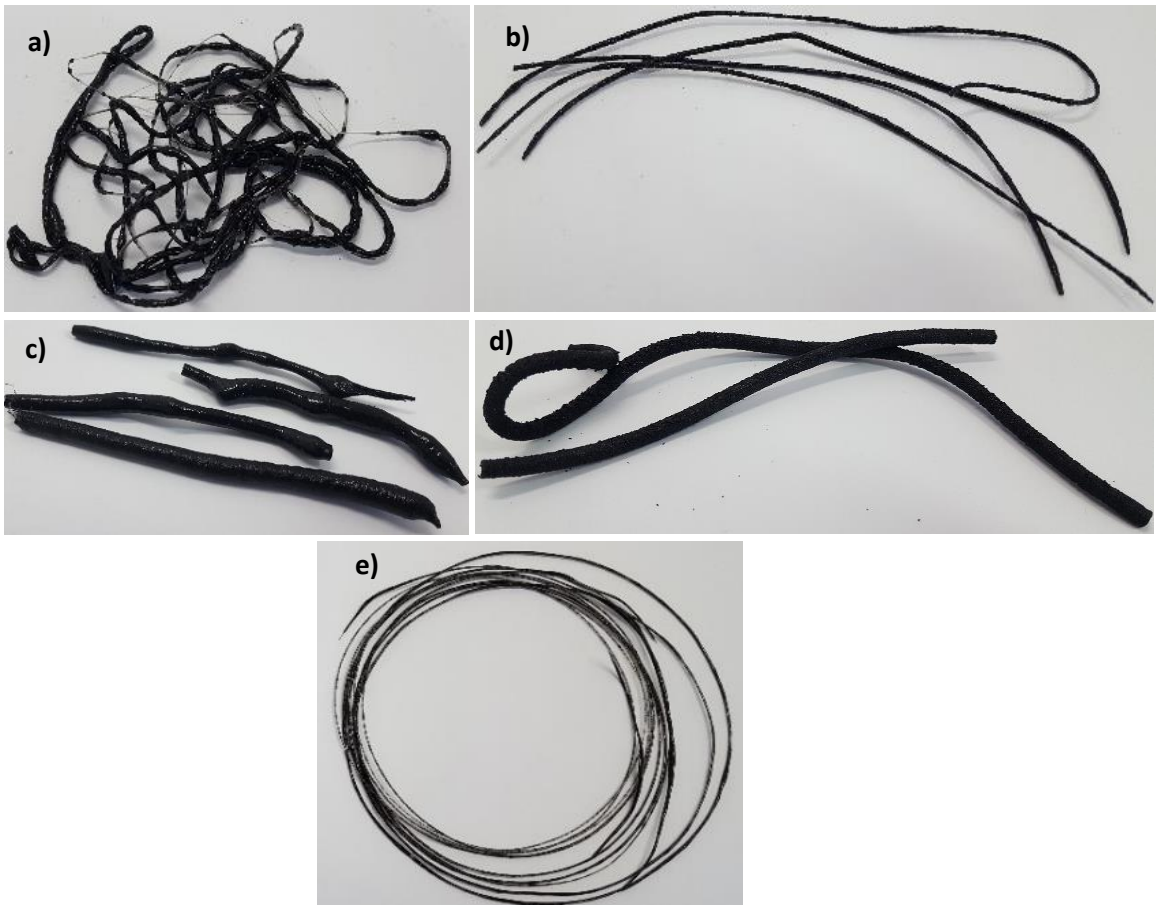

Figure 3.7 – Different composite mixtures extruded into filament form: a) 10 wt.% rubber; b) 20 wt.% rubber; c) 40 wt.% rubber; d) 60 wt.% rubber; e) 20 wt.% rubber + 2 wt.% glycerol (filament F1). Filament F1 was chosen to be applied in additive manufacturing.

For filaments with 10, 20, 40 and 60 wt.% rubber, it was extremely hard to control the diameter dimensions and to obtain a proper filament to use in additive manufacturing. Filament prepared with 20 wt.% rubber + 2 wt.% glycerol presented a good flexibility, however it was still hard to control the filament diameter. Moreover, the filaments with high rubber content were very brittle and impossible to roll into a skein. The experimental results here reported are well in accordance with our theoretical predictions in Figure 3.1; our theoretical calculations show that the properties of PLA are considerable affected by the presence of the rubber fillers and this variation is accentuated up to 10 % in volume of rubber and after that the variation of the calculated mechanical properties is almost unnoticeable. In addition, the theoretical density of the composites, starts to be affected only after 20 % in volume. For these reasons, 20 % mass fraction of granulate was selected for our

further studies and it was decided to add glycerol (2 wt.%) as plasticizer to enhance the flexibility of the filament (Figure 3.6 e). Under these conditions, it was possible to achieve a filament with enhanced properties for the printing. It should be noticed that the homogeneity of the filament was not optimal, still being possible to distinguish the rubber granulates. This observation may be related to the thermal stability of the granulates, which up to 300°C do not suffer any modification. As the mixture is done at 190°C, the granulates maintain their initial appearance, not mixing entirely with PLA. This observation should be taken in consideration, since it may affect the printing process.

Despite the defects, the filament possesses the necessary features to be applied in additive manufacturing. In order to proceed, a study of the variability of its diameter was performed and is represented in Figure 3.8.

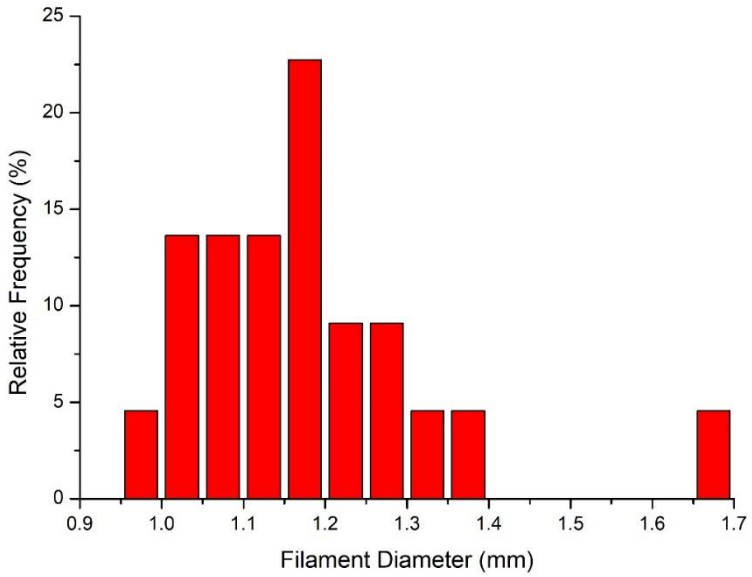

Figure 3.8 – Variability of the filament F1 diameter extruded with spooling on. This study was performed by measuring the filament diameter every 2 cm. This filament presented a mean value of 1.17 mm of diameter and a median value of 1.16 mm.

Filament F1 presented a mean value of 1.17 mm of diameter and a median value of 1.16 mm, which is a filament way too thin that did not work well with the feeding system that was prepared for filaments with a bigger diameter (between 1.75 and 2 mm). However, this filament was still used for some printing attempts, more in particular, for printing an 8 cm^3 cube, represented in Figure 3.10.

However, we consider that it is yet necessary to retain that there is a necessity to improve the mixture homogenization control and to better control the filament diameter, to obtain the best possible results.

Since there was the necessity of a filament with higher diameter, a new mixture with the same composition (20 wt.% rubber + 2 wt.% glycerol) and a new filament extrusion were performed, with the same conditions, but, this time, with the spooling feature of the NEXT extruder turned off. Under this condition the filament was spooled out of the extruder manually as shown in Figure 3.9. In this way it was possible to achieve a filament with high diameter, while preserving the flexibility (Figure 3.9).

However, as previously, it was not possible to obtain a homogeneous filament with constant diameter value. In Figure 3.10, is represented the variability of the diameter of this new filament. This variability study was performed by measuring the filament diameter every 2 cm. This filament presented a mean value of 1.97 mm and a median value of 1.96 mm, values that are in the desired diameter range.

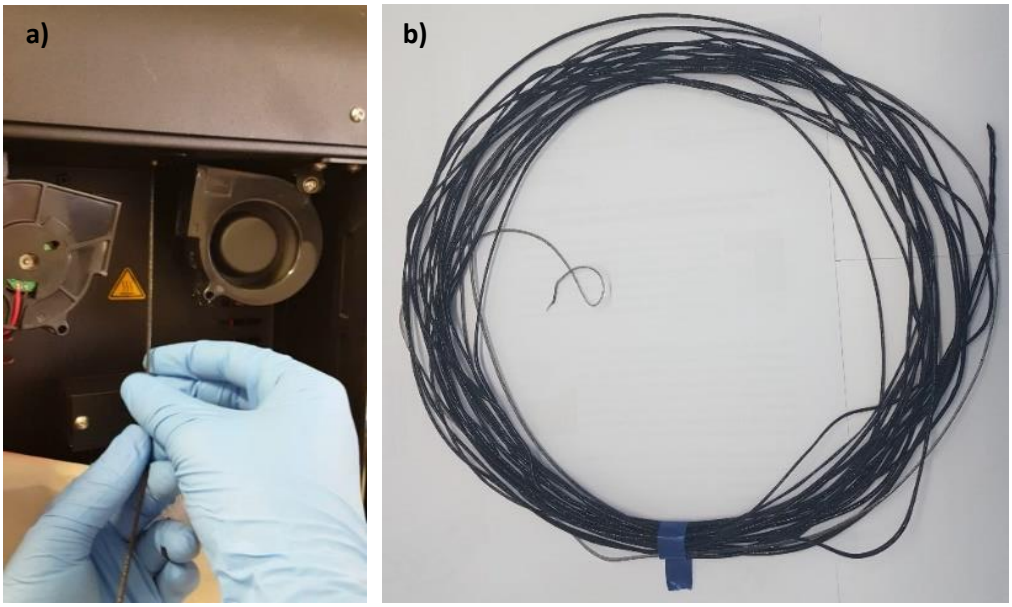

Figure 3.9 – Filament F2 extruded with spooling off: a) manual extrusion and b) final filament.

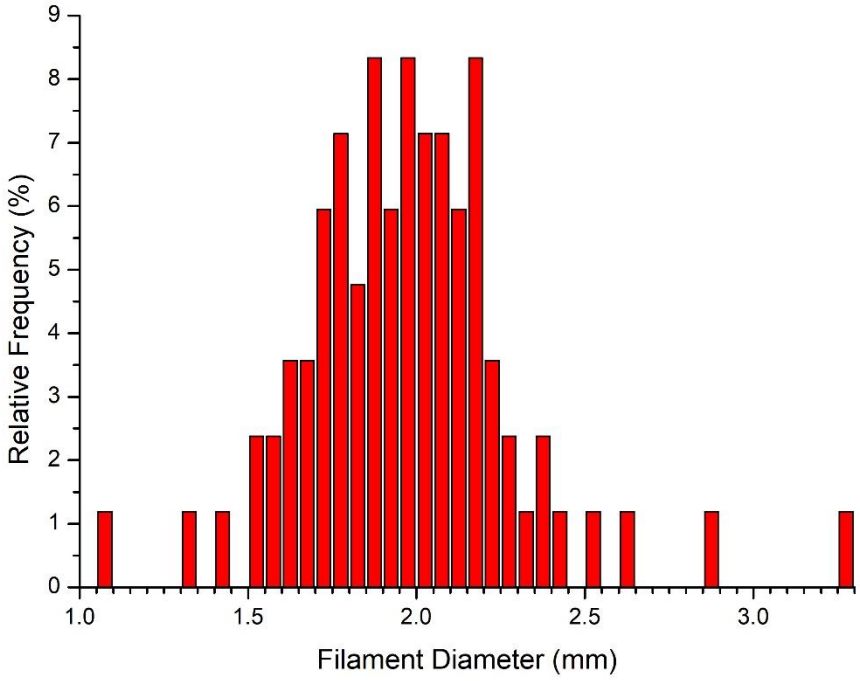

Figure 3.10 – Variability of the filament F2 diameter extruded with spooling off. This study was performed by measuring the filament diameter every 2 cm. This filament presented a mean value of 1.97 mm and a median value of 1.96 mm.

It is important to enhance that, during the filament extrusion, there is a period where only liquid mixture is coming out the extruder, for both manual and automatic spooling. This liquid may be related with glycerol in excess, not properly mixed with the other components.

To improve the homogeneity of the filament, some improvement of the mixtures must be done. For example, grinding the cryogenic rubber granulates, to reduce its size and to facilitate its incorporation in the PLA matrix; to cleave the sulfur chemical bonds.

3.5. ADDITIVE MANUFACTURING

According to the experimental observations, the printer parameters (temperature and diameter nozzle) were carefully selected. The first printing attempts were a $8\,cm^3$ cube, represented in Figure 3.11. These attempts were performed with the filament F1.

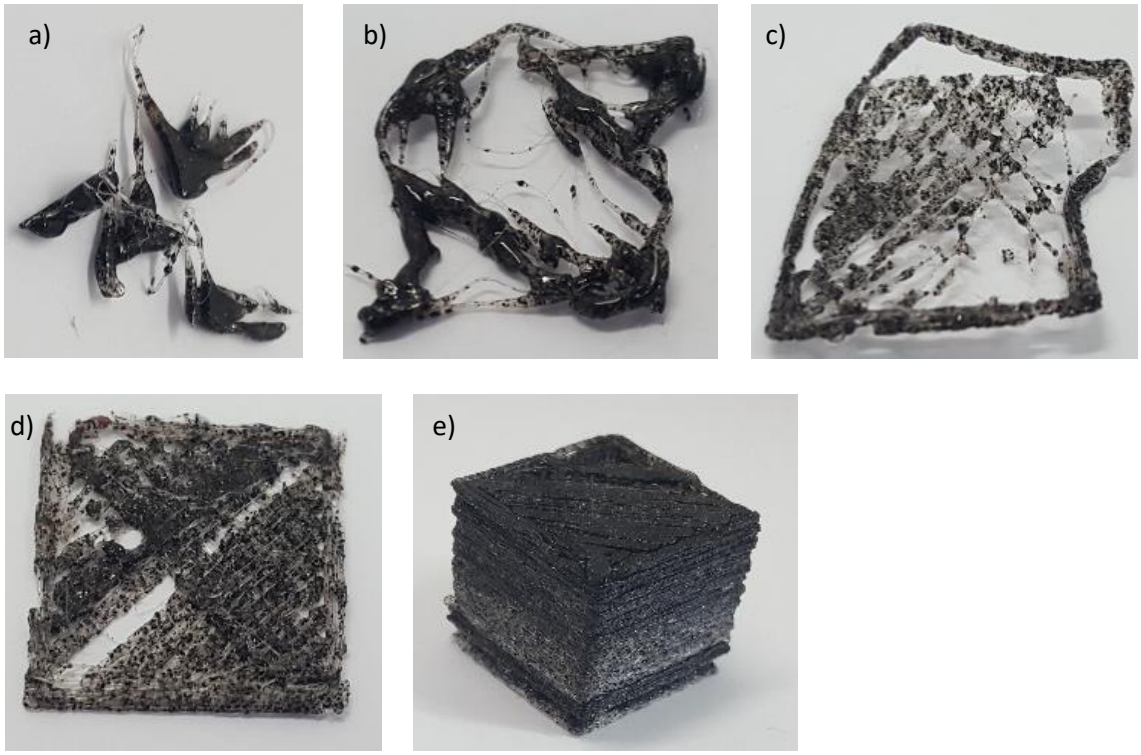

Figure 3.11 - The first printing attempts were an 8 cm³ cube. Different temperatures and nozzle diameters were tested: a) T=190°C, 0.8 mm nozzle; b) T=180°C, 0.8 mm nozzle; c) T=170°C, 0.8 mm nozzle; d) T=170°C, 0.6 mm nozzle; e) T=170°C, 0.6 mm nozzle. The most suitable parameters were defined as T=170°C and a 0.6 mm nozzle diameter, ensuring a continuous printing.

Only for a temperature of T = 170°C and with a nozzle diameter of 0.6 mm (d and e) it was possible to obtain the 8 cm^3 cube (Figure 3.11). In both cases a) and b), the temperature was too high, and the material extruded was too liquid, so a lower temperature was needed. In c), we got closer to the desired 8 cm^3 cube, however there was a necessity of decreasing the nozzle diameter (from 0.8 to 0.6 mm) in order to ensure a continuous feeding and to make sure that the differences in the filament diameter doesn't influence the printing in a significant way.

After these experimental observations, the most suitable parameters were defined as $T = 170°C$ and a $0.6\ mm$ nozzle diameter. The filament, as said before, had a too low diameter value what made very difficult the printing, being necessary to push the filament to feed the printer head.

Using the filament F2, some attempts to 3D print the desired “egg box type” panel took place, according to the following CAD model (Figure 3.12).

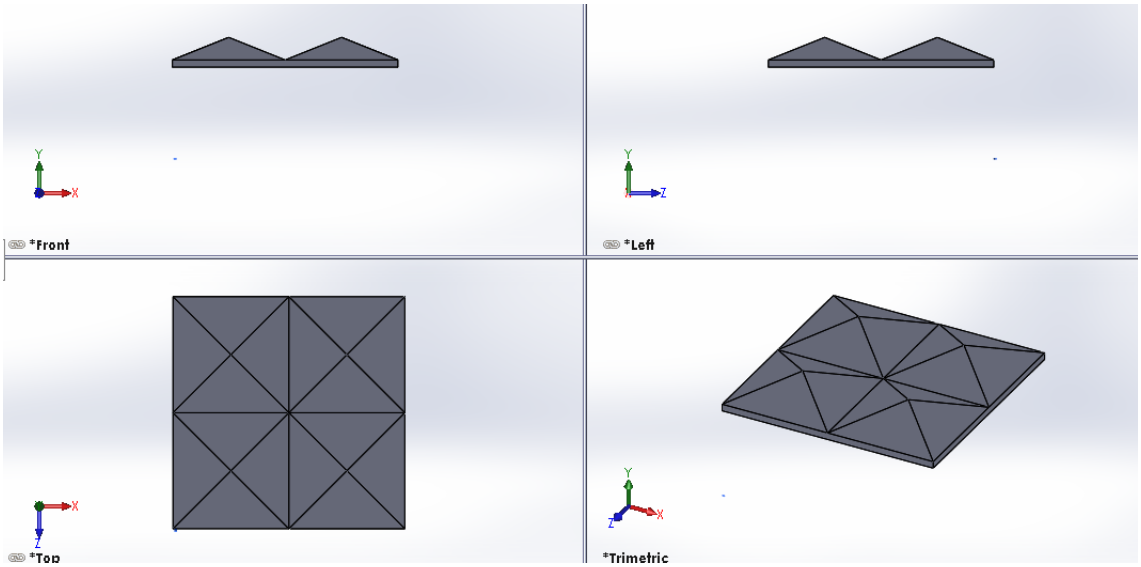

Figure 3.12 – CAD model of the “egg box type” panel designed with a quadrangular base of 5 cm side, with four quadrangular pyramids of 1 cm of height.

The panel was designed with a quadrangular base of 5 cm side, with four quadrangular pyramids of 1 cm of height on the top (Figure 3.12).

During the first printing attempt, the printer had to be stopped after a while since some filament parts got stuck in the printing head, due to the variation in the filament diameter. The result of this first attempt is presented in Figure 3.13.

Figure 3.13 – First printing attempt of an "egg box type" panel designed with a quadrangular base of 5 cm side, with four quadrangular pyramids of 1 cm of height. Panel printed with filament F2, with a 0.6 mm nozzle diameter and an extrusion temperature of T = 170°C.

Some changes in the printing head were performed (enlarging the hole through where the filament passes), to make sure that all filament could pass and be extruded without getting stuck and print the panel.

The nozzle diameter used was 0.6 mm and the temperature T = 170°C. The Bed was heated up to T = 65°C and the fan speed set at 25%. A primary layer height of 0.320 mm was used, with an extrusion multiplier of 1 and an interior fill of 20%. The default printing speed was set at 50 mm/s, with an outline underspeed of 50% and with a solid infill underspeed of 80%. The resulting panels are represented in Figure 3.14.

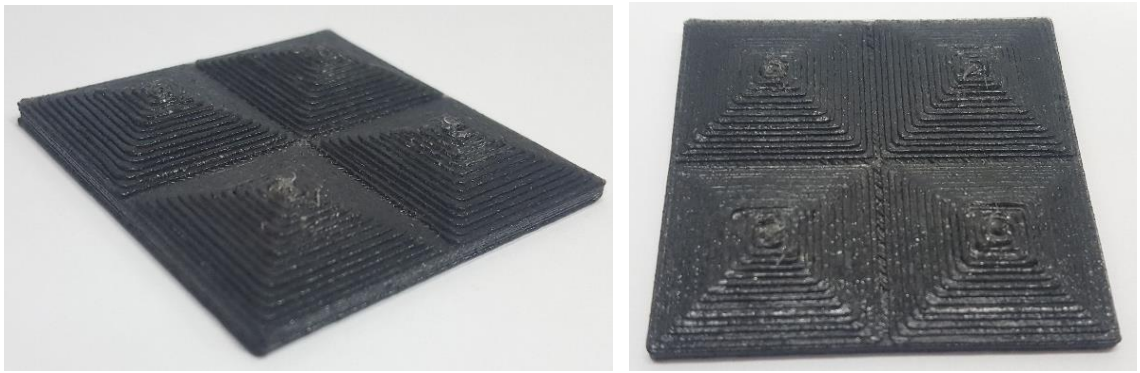

Figure 3.14 – "Egg box type" panel designed with a quadrangular base of 5 cm side, with four quadrangular pyramids of 1 cm of height. Panel printed with filament F2, with a 0.6 mm nozzle diameter and an extrusion temperature of T = 170°C.

After printing the “egg box type” panel, it was time to perform the acoustic characterization of our composite material. To perform that, 3 round samples were printed.

Recalling Table 2.3, the identification and characteristics of the round printed samples are described in Table 3.5.

Table 3.5 – Identification and characteristics of the printed samples (A1, A2 and A3) for acoustic characterization.

Sample	Characteristics
A1	Flat PLA sample
A2	Flat sample printed with filament F2
A3	“Egg box type” sample printed with filament F2

Samples A1 and A2 were designed to be round flat samples, with 5 cm diameter and 3 cm of height, while sample A3 was designed to be a round sample with an “egg box type” topography, also with 5 cm diameter and 3 cm of height. The CAD model of both samples are presented next: samples A1 and A2 (Figure 3.15) and sample A3 (Figure 3.16).

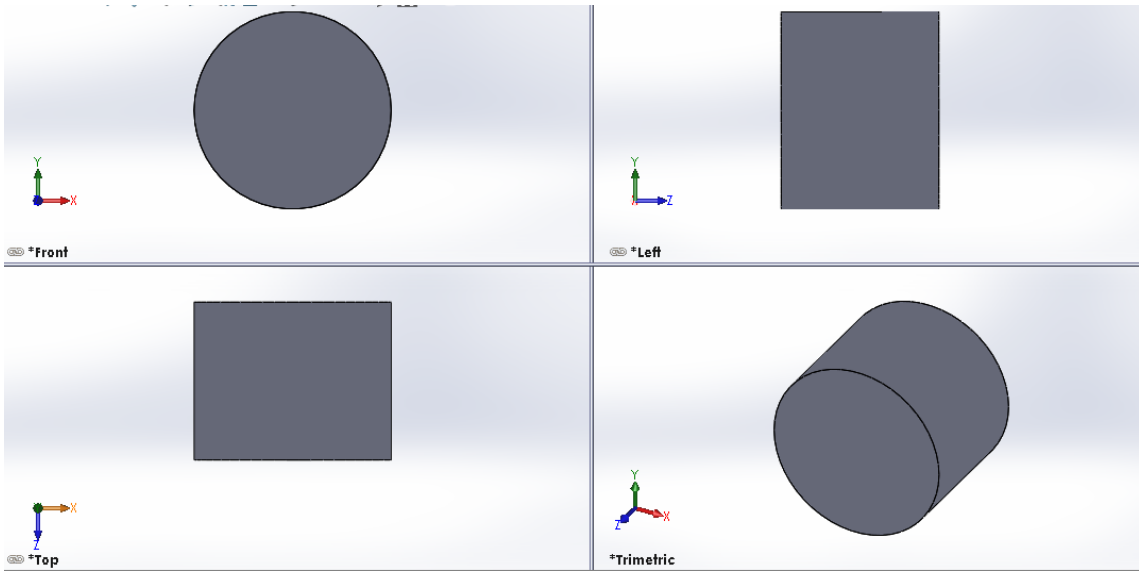

Figure 3.15 – CAD model of samples A1 and A2. Round flat samples with 5 cm of diameter and 3 cm of height.

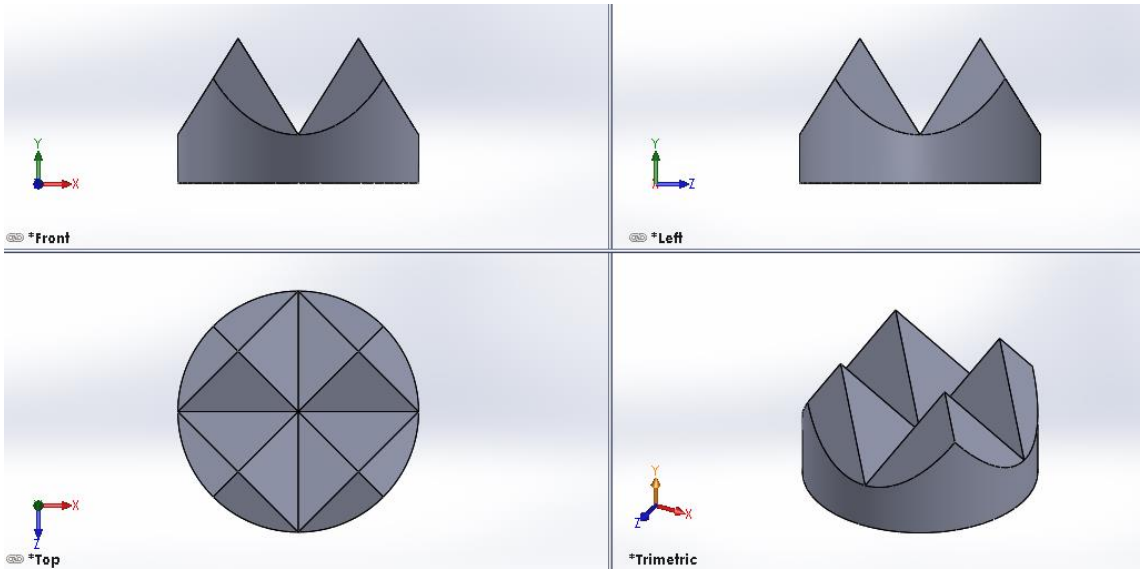

Figure 3.16 – CAD model of sample A3. Round sample with "egg box type" topography with 5 cm diameter and 3 cm of height.

The round sample, A1, printed for acoustic characterization, was performed entirely with PLA, while samples A2 and A3 were performed with the filament F2 (Table 3.5).

The printing of sample A1 was performed with a 0.6 mm nozzle diameter and with an extrusion temperature of T = 200°C. The bed was at a temperature of T = 65°C and the fan speed set at 25 %. A primary layer height of 0.320 mm was used, with an extrusion multiplier of 1 and an interior fill of 20 %. The default printing speed was set at 50 mm/s, with an outline underspeed of 50 % and with a solid infill underspeed of 80 %.

The printing parameters for samples A2 and A3 were the same, apart from the extrusion temperature that was set at T = 170°C.

Prepared samples for acoustic characterization are shown in the following figures, according to the CAD models (Figure 3.15 and Figure 3.16): sample A1 (Figure 3.17), sample A2 (Figure 3.18) and sample A3 (Figure 3.19).

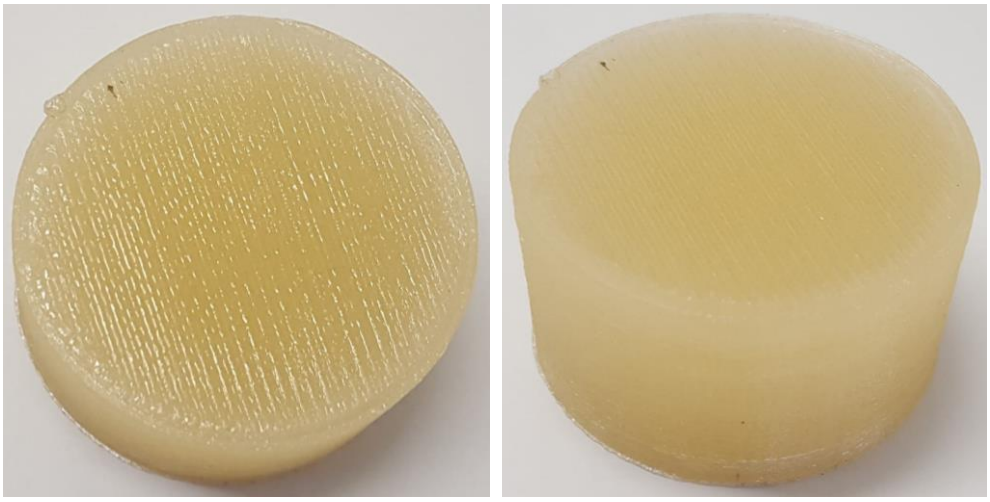

Figure 3.17 – Sample A1 – Flat PLA sample.

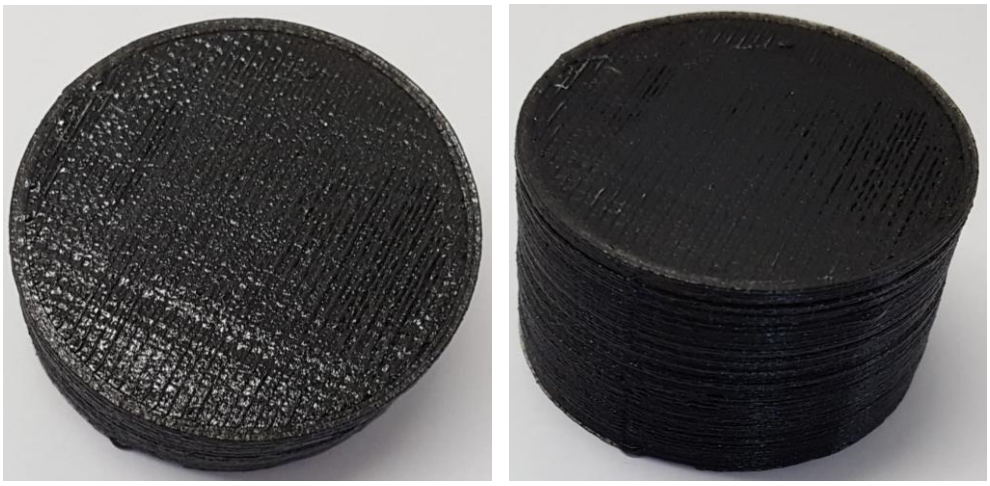

Figure 3.18 – Sample A2 – Flat sample printed with filament F2.

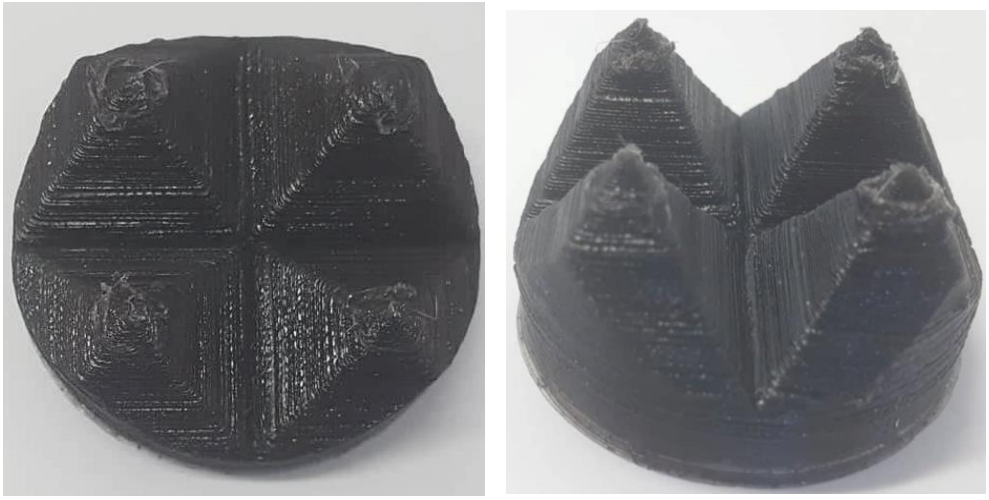

Figure 3.19 – Sample A3 – "Egg box type" sample printed with filament F2.

However, just before the acoustic characterization of the printed samples, their density was measured, by means of the Archimedes' method, and compared with the theoretical prediction of the composites' density behavior.

3.6. DENSITY DETERMINATION

The mass of both samples A1 and A2 were measured previously, being registered that sample A1 presented a mass of $m = 60.40\ g$, while sample A2 presented a mass of $m = 63.77\ g$.

The Archimedes' method was performed, and the mass values of the immersed samples obtained were: $m_i = 11.50\ g$ (sample A1) and $m_i = 11.81\ g$ (sample A2).

Using Equation 2.4, the density of both samples was determined as follows:

$$\rho_{sample\ A1} = \frac{60.40}{60.40 - 11.50} \times 1 = 1.235\ g/cm^3$$

$$\rho_{sample\ A2} = \frac{63.77}{63.77 - 11.81} \times 1 = 1.227\ g/cm^3$$

The density obtained for sample A1 was $1.235\ g/cm^3$ and, for sample A2 was $1.227\ g/cm^3$. These results are well in accordance with the theoretical prediction presented in Figure 3.1, since it was expected that sample A2, containing 20 wt.% rubber, would present a lower density than sample A1, performed entirely with PLA.

3.7. ACOUSTIC CHARACTERIZATION

By means of the wave impedance tube method, the absorption coefficient results of the sample A1 and A2 were obtained and are, in Figure 3.20, analyzed and discussed.

For lower frequency values, both samples A1 and A2 presented similar absorption coefficient values, however, for higher frequency values, the absorption coefficient values obtained were quite different. For example, for a frequency of around 3400 Hz, sample A1 presented an absorption coefficient of 0.25, while sample A2 presented an absorption coefficient of only 0.075. It is also noticeable that the higher values of absorption coefficient obtained were for both low and high frequencies.

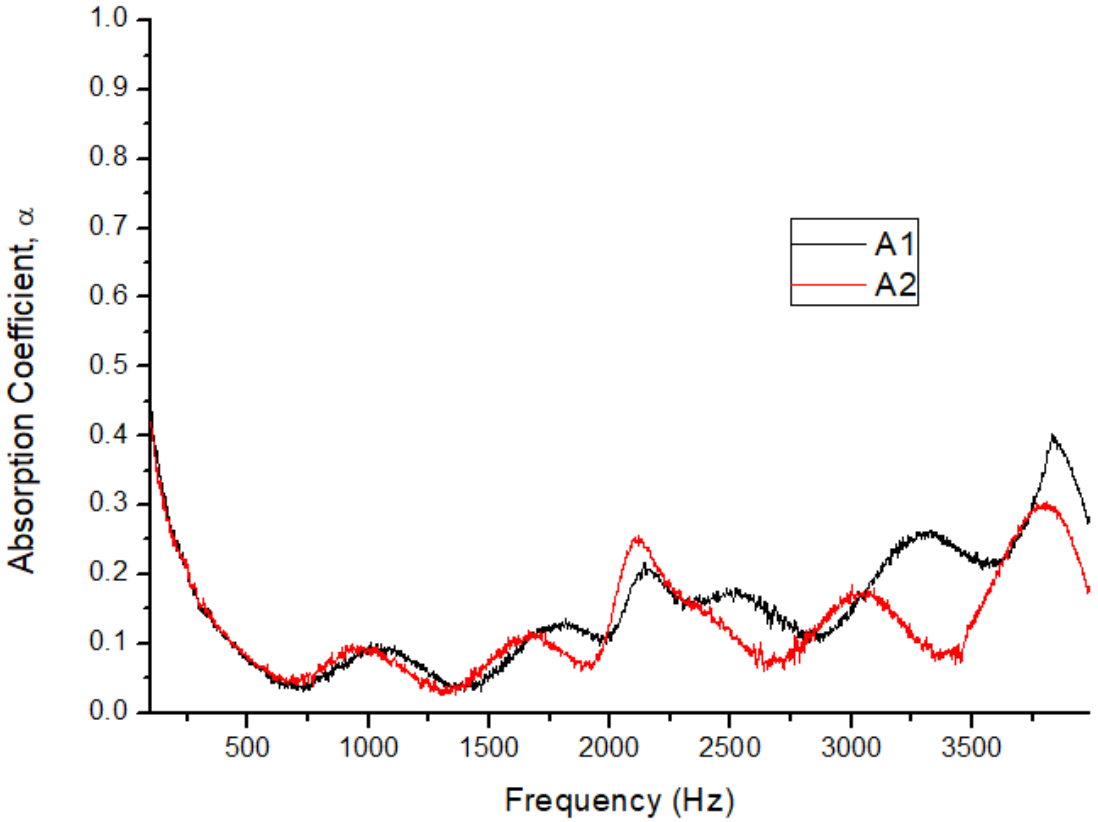

Figure 3.20 – Comparison between the acoustic absorption results of samples A1 and A2. For lower frequencies, samples A1 and A2 presented similar absorption coefficient results, however, for higher frequencies, the absorption coefficient values were quite different. Samples A1 and A2 are reflective materials.

Analyzing these results, we conclude that, for both samples, we are in a presence of a reflective material (does not allow the entrance of the sound waves) probably due to the stiff nature and low porosity of the samples. Notice that it was not possible to acoustically characterize sample A3, due to its irregular shape. The sample's topology does not fit in this method, since its irregular shape and reflective characteristics will break the plane wave generated, not giving reliable results.

After that, a comparison of both samples A1 and A2 with a mineral wool sample was performed. The mineral wool sample is an example of an absorbent material widely used nowadays in acoustic solutions. This comparison is set in Figure 3.21.

The mineral wool sample presented an absorption coefficient of around 0.2 for a frequency of 100 Hz, however, this value drastically increased reaching an absorption coefficient of almost 1.

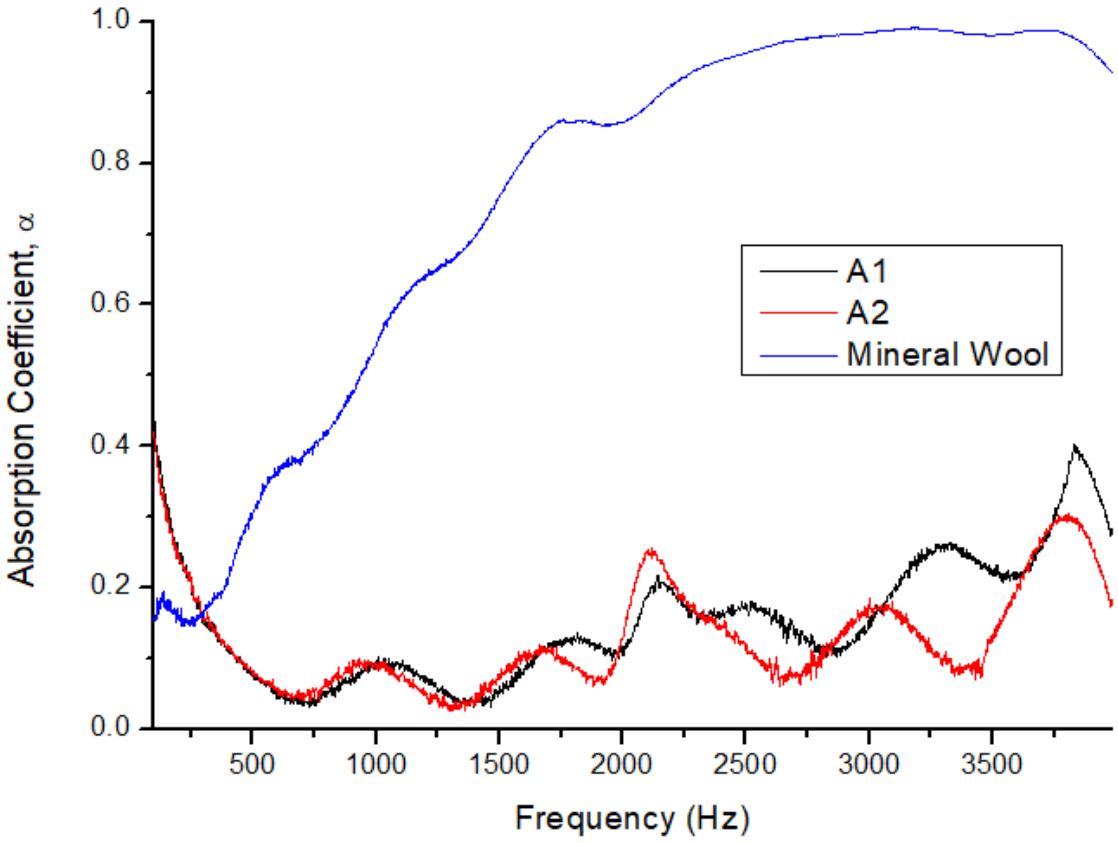

Figure 3.21 - Comparison between the acoustic absorption results of samples A1, A2 and a mineral wool sample (example of an absorbent material). A tridimensional structure with porosity is necessary to improve the absorption coefficient value of our samples.

The mineral wool presented in this comparison had the same dimensions as samples A1 and A2, however it was spongy and malleable, with high porosity. In order to improve the results obtained for samples A1 and A2, a tridimensional structure with porosity is necessary, to allow the sound waves to enter the samples, improving the absorption coefficient value.

4. CONCLUSIONS AND FUTURE WORK

4. CONCLUSIONS AND FUTURE WORK

In this work, rubber based polymeric composites of recycled tires for additive manufacturing were exploited, being an acoustic panel, the prototype to be tested. To meet the challenge, a composite filament containing PLA and recycled rubber was developed.

Firstly, a theoretical prediction of the composites' behavior was performed by means of the software CES Selector 2017, and it was concluded that the mechanical properties of the PLA matrix (tensile strength, yield strength, Young modulus and compressive strength) decreased with the rubber addition, being the variation more accentuated for low percentages of rubber, reaching a minimum value for around 10 % in volume, being almost constant after this value. Also, the density variation was predicted, pointing to a constant density value until around 20 % in volume, perceiving a substantial decrease between 20 and 30 % in volume and, afterwards, a density stability for higher percentages of rubber, evidencing a slight increase of this value for increasingly high rubber percentages.

After that, the raw material (DC-8000) characterization was performed through different techniques: SEM/EDS, FTIR and DSC/TGA.

The analysis of the SEM micrographs allowed us to conclude that, as expected, the grains of the raw material presented irregular shapes, flat morphology and a smooth surface, as it is typical in cryogenic rubber granulates. Through EDS analysis, it was possible to detect the presence of elements like carbon, sulfur, silica, zinc, oxygen, calcium, aluminum and iron, as it was also expected.

The FTIR spectroscopy analysis was performed to verify qualitatively the functional groups present on the rubber samples and to provide new data about the raw material to RECIPNEU. As it was expected, it was possible to see the vibrations corresponding to the functional groups present in the tires such the ones assigned to the rubber and functional groups related with the rubber vulcanization.

The DSC/TGA analysis allowed us to conclude that the raw material is almost stable up to 300°C, where the weight loss is almost negligible. Above 300°C and up

to 500°C, a huge drop of the granulate mass of around 60 % is visible (may be associated to the cleavage of the sulfur bonds with consequent combustion of the organic groups of the polymeric part of the rubber). It was possible to observe an exothermic peak at 365°C related with initiation of the decomposition of the rubber granulates and, an endothermic peak around 420°C, considered to be caused by partial oxidation of carbon black.

After the raw material characterization, the preparation of the composite formulation took place and mixtures of PLA and rubber were prepared, with rubber percentages, in mass, between 10 and 60 %. A rubber percentage of 20 wt.% was also tested with glycerol (2 wt.%) as additive.

All mixtures were extruded in filament form, however it was concluded that only the mixture performed with 20 wt.% of rubber and 2 wt.% glycerol presented the necessary features to be applied in additive manufacturing.

With the filament obtained, some attempts to print an “egg box type” panel were performed, being the desired object successfully obtained with a nozzle diameter of 0.6 mm and a temperature of T = 170°C.

Finally, to perform the acoustic characterization, 3 round samples with 5 cm of diameter and 3 cm of height were printed: sample A1 (flat PLA sample), sample A2 (flat sample printed with filament F2) and sample A3 (“egg box type” sample printed with filament F2). The acoustic characterization was performed by means of the wave impedance tube method.

Analyzing the acoustic results obtained, it was possible to conclude that both samples A1 and A2 are reflective materials, not allowing the entrance of the sound waves, probably due to their stiff nature and low porosity. It was also possible to conclude that, to achieve better acoustic results, these samples need to have a tridimensional structure with porosity, allowing the sound waves to enter in the sample, improving the absorption coefficient results.

Additionally, this thesis opens an avenue of future studies, following the circular economy trend, by giving new lives to the nowadays wastes.

Future Work:

1. Improving the mixture homogenization by, for example, grinding the cryogenic rubber granulates previously to the mixing.
2. Improving the percentage of rubber waste to be added to the composite formulation.
3. Improving both filament homogenization and diameter control, improving consequently the quality of the printed pieces.
4. Improving both design and characteristics of the printed pieces, reducing the reflection of the sound wave and enhancing the absorption.

5. REFERENCES

5. REFERENCES

[1] "http://www.michelin.pt/pneus-turismo/conselhos/tudo-sobre-o-pneu/o-que-compoe-um-pneu." [Accessed: 17-May-2018].

[2] V. L. Shulman, *Tyre Recycling, Vol.15, 2004*.

[3] C. S. S. R. Kumar and A. M. Nijasure, "Vulcanization of Rubber," *Resonance*, pp. 2–3, 1997.

[4] "https://www.khanacademy.org/test-prep/mcat/physical-sciences-practice/physical-sciences-practice-tut/e/elasticity-and-kinetics-of-vulcanized-rubber." .

[5] P. Silva Santos, "Aproveitamento Industrial da Borracha Reciclada de Pneus Usados," Universidade do Minho, 2006.

[6] "http://www.valorpneu.pt/." .

[7] "http://www.etrma.org/." .

[8] "http://www.scraptirenews.com/." [Online]. Available: http://www.scraptirenews.com/crumb.php#prettyPhoto. [Accessed: 03-May-2018].

[9] D. Lo Presti, "Recycled Tyre Rubber Modified Bitumens for road asphalt mixtures : A literature review," *Constr. Build. Mater.*, vol. 49, pp. 863–881, 2013.

[10] Recipneu, "Cryogenic rubber infill by Recipneu," Sines.

[11] A. R. Khaloo, M. Dehestani, and P. Rahmatabadi, "Mechanical properties of concrete containing a high volume of tire – rubber particles," *Waste Manag.*, vol. 28, no. 12, pp. 2472–2482, 2008.

[12] M. J. Swift, P. Brisï, and K. V Horoshenkov, "Acoustic absorption in re-cycled rubber granulate," *Appl. Acoust.*, vol. 57, pp. 203–212, 1999.

[13] "http://www.recipneu.com/." [Accessed: 25-January-2018].

[14] J. Zhao, X. Wang, J. M. Chang, Y. Yao, and Q. Cui, "Sound insulation property of wood – waste tire rubber composite," *Compos. Sci. Technol.*, vol. 70, no. 14, pp. 2033–2038, 2010.

[15] C. Buratti, E. Belloni, E. Lascaro, G. Anna, and P. Ricciardi, "Sustainable panels with recycled materials for building applications : environmental and acoustic characterization," *Energy Procedia*, vol. 101, no. September, pp. 972–979, 2016.

[16] Z. Hong, L. Bo, H. G. Ã, and H. Jia, "A novel composite sound absorber with recycled rubber particles," *J. Sound Vib.*, vol. 304, pp. 400–406, 2007.

[17] H. Yang, D. Kim, Y. Lee, H. Kim, J. Jeon, and C. Kang, "Possibility of using waste tire composites reinforced with rice straw as construction materials," *Bioresour. Technol.*, vol. 95, pp. 61–65, 2004.

[18] R. Maderuelo-sanz, A. V Nadal-gisbert, J. E. Crespo-amorós, and F. Parres-garcía, "A novel sound absorber with recycled fibers coming from end of life tires (ELTs)," *Appl. Acoust.*, vol. 73, pp. 402–408, 2012.

[19] D. R. Raichel, *The science and applications of acoustics*, Second Edi. 2006.

[20] K. Heutschi, *Lecture Notes on Acoustics I*. Zurich, 2016.

[21] V. O. Knudsen and C. M. Harris, *Acoustical Designing in Architecture*, Fifth edit. American Institute of Physics, 1988.

[22] “Hull, C.W., Apparatus for production of three-dimensional objects by stereolithography. 1986.”

[23] X. Wang, M. Jiang, Z. Zhou, J. Gou, and D. Hui, “3D printing of polymer matrix composites : A review and prospective,” *Compos. Part B*, vol. 110, pp. 442–458, 2017.

[24] “Based on http://sadanaresearch.com/3d-printing-research/.” [Online]. Available: http://sadanaresearch.com/3d-printing-research/. [Accessed: 11-Apr-2018].

[25] S. H. Masood and W. Q. Song, “Development of new metal / polymer materials for rapid tooling using Fused deposition modelling,” *Mater. Des.*, vol. 25, pp. 587–594, 2004.

[26] M. Nikzad, S. H. Masood, and I. Sbarski, “Thermo-mechanical properties of a highly filled polymeric composites for Fused Deposition Modeling,” *Mater. Des.*, vol. 32, no. 6, pp. 3448–3456, 2011.

[27] A. N. R. da Costa, “Nanocompósitos de matriz polimérica para impressão 3D,” Univesidade de Aveiro, 2016.

[28] K.K.Car, J. K. Pandey, and S. Rana, *Handbook of Polymer Nanocomposites. Processing, Performance and Application*, Vol B. Berlin: Springer, 2015.

[29] F. Yemisci, S. Yesil, and A. Aytan, “Improvement of the flame retardancy of plasticized poly (lactic acid) by means of phosphorus - based flame retardant fillers,” 2017.

[30] X. Tian, T. Liu, C. Yang, Q. Wang, and D. Li, “Interface and performance of 3D printed continuous carbon fiber reinforced PLA composites,” *Compos. Part A*, vol. 88, pp. 198–205, 2016.

[31] D. Drummer, S. C. Cuéllar, D. Rietzel, and D. Rietzel, “Suitability of PLA / TCP for fused deposition modeling,” *Rapid Prototyp.*, 2012.

[32] O. S. Carneiro, A. F. Silva, and R. Gomes, “Fused deposition modeling with polypropylene,” *Mater. Des.*, vol. 83, pp. 768–776, 2015.

[33] CES Selector. Version 2017. Granta Design, 2017.

[34] A. Lopes, “Material Characterization II -X-ray Diffraction,” 2016.

[35] Thermo Nicolet, “Introduction to Fourier Transform Infrared Spectrometry,” 2001.

[36] L. H. Sperling, *Introduction to Physical Polymer Science*, Fourth. USA: John Wiley & Sons, Inc., 2006.

[37] TA Instruments, “TA Instruments Differential Scanning - Operating Instructions.”

[38] Perkin Elmer, “Thermogravimetric analysis,” 1960.

[39] “https://www.brabender.com/en/chemical/products/measuring-mixer/.” .

[40] “http://3devo.com/next-filament-extruder/.” .

[41] Solidworks. Version 2017.

[42] A. B. Spierings, M. Schneider, and R. Eggenberger, “Comparison of density measurement techniques for additive manufactured metallic parts,” *Rapid Prototyp.*, vol. 5, no. July 2010, pp. 380–386, 2011.

[43] “ASTM E1050-98, Standard Test Method for Impedance and Absorption of Acoustical Materials Using A Tube , Two Microphones and A Digital Frequency Analysis System,” *ASTM Int.*, p. West Conshohocken, PA, 1998.

[44] “http://www.grantadesign.com/education/edupack/.” [Accessed: 02-February-2018].

[45] L. Xiao, B. Wang, G. Yang, and M. Gauthier, “Poly (Lactic Acid) -Based Biomaterials : Synthesis , Modification and Applications,” 2012.

[46] “https://webbook.nist.gov/chemistry/vib-ser/.” .

[47] A. Zanchet, L. N. Carli, M. Giovanela, R. N. Brandalise, and J. S. Crespo, “Use of styrene butadiene rubber industrial waste devulcanized by microwave in rubber composites for automotive application,” *Mater. Des.*, vol. 39, pp. 437–443, 2012.

[48] R. Sacher, D. Macaione, and R. Singler, “Thermal Analysis Characterization of Elastomers and Carbon Black Filled Rubber Composites for Army Applications,” 1985.

[49] M. Rossi and M. Pagliaro, “Glycerol : Properties and Production,” in *The Future of Glycerol: New Uses of a Versatile Raw Material*, 2008, pp. 1–18.

[50] “http://www.anet3d.com/English/3D_Printer/106.html.” .